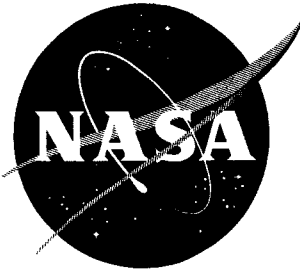


~~CONFIDENTIAL~~ NASA:TM X-542

NASA TM X-542



# TECHNICAL MEMORANDUM

X-542

Hard copy (HC) 12.00

Microfiche (MF) 57

## LOW-SPEED INVESTIGATION OF HIGH-LIFT AND LATERAL CONTROL DEVICES ON A SEMISPAN VARIABLE-SWEEP WING HAVING AN OUTBOARD PIVOT LOCATION

By William P. Henderson and Alexander D. Hammond

Langley Research Center  
Langley Field, Va.

DECLASSIFIED: Effective 2-5-65  
Authority: F.G. Drobka (ATSS-A)  
memo dated 3-25-65: AFSDO-5197

DECLASSIFIED BY AUTHORITY OF NASA  
CLASSIFICATION CHANGE NOTICES NO. 11  
DATED 7-21-65 ITEM NO. 11

FACILITY FORM 602

N65-23918  
(ACCESSION NUMBER)

39  
(PAGES)

(NASA CR OR TMX OR AD NUMBER)

(THRU)

(CODE)

01  
(CATEGORY)

NATIONAL AERONAUTICS AND SPACE ADMINISTRATION

WASHINGTON

May 1961

~~CONFIDENTIAL~~

1Y

~~CONFIDENTIAL~~  
DECLASSIFIED

NATIONAL AERONAUTICS AND SPACE ADMINISTRATION

TECHNICAL MEMORANDUM X-542

DECLASSIFIED BY AUTHORITY OF NASA  
CLASSIFICATION CHANGE NOTICES NO. 14  
DATED 11-21-85 ITEM NO. 11

LOW-SPEED INVESTIGATION OF HIGH-LIFT AND

LATERAL CONTROL DEVICES ON A SEMISPAN VARIABLE-SWEEP WING

HAVING AN OUTBOARD PIVOT LOCATION\*

By William P. Henderson and Alexander D. Hammond

SUMMARY

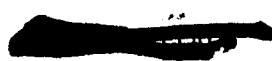
USE CARD IN BACK

An investigation was made to determine the effect of leading-edge and trailing-edge-flap deflections and spoiler-slot-deflector projections on the high-lift and lateral control characteristics of a semispan variable-sweep-wing configuration. The high-lift characteristics were obtained on three types of trailing-edge-flap devices, a single-slotted flap, a spoiler-slot-deflector high-lift device, and a double-slotted flap, each in conjunction with a leading-edge flap. The lateral control characteristics were obtained by the use of spoiler-slot-deflector projections on both the wing with the flaps deflected and with the flaps neutral.

The results indicated that a nearly linear increase in lift coefficient was obtained with increasing flap deflection up to approximately 30° deflection for the single-slotted flap and for the spoiler-slot-deflector configuration and up to approximately 40° for the double-slotted flap. Further increases in flap deflection resulted in only small increases in lift effectiveness and were accompanied by rather large increases in drag. Rather abrupt unstable variations of pitching moment with lift occurred at moderate lift coefficients for the wing with trailing-edge flaps deflected. Increasing deflections of the leading-edge flap progressively delayed this unstable variation to higher lift coefficients.

The effect of increasing the spoiler-slot-deflector projections as a lateral control device was to decrease the lift coefficient, increase the drag coefficient, and produce a positive increment of pitching-moment coefficient with no appreciable change in the slope of the pitching-moment curves. Adequate rolling moment and favorable yawing moment were produced by the higher spoiler-slot-deflector projections throughout the usable angle-of-attack range.

\*Title, Unclassified.



L  
1  
1  
5  
2  
7

CONFIDENTIAL

## INTRODUCTION

Considerable interest is being shown in the use of variable-sweep wings as a means of providing an aircraft with multimission capabilities. These capabilities include: low-speed ferry or loiter; high-altitude supersonic cruise, intercept, or attack; and low-level attack. Reference 1 summarizes the results of a wind-tunnel study aimed toward the development of a variable-sweep-wing configuration having satisfactory stability and control characteristics throughout the wing sweep range. Reference 2 presents detailed subsonic and transonic aerodynamic data on the configuration that evolved from this study. However, since simplified models were used in references 1 and 2 it appeared desirable to obtain aerodynamic data on models more representative of current fighter airplanes. A summary of the research on these configurations which have some or all of the capabilities just mentioned is presented in reference 3.

In view of the acceptable longitudinal stability characteristics obtained on the variable-sweep-wing configurations of reference 3 it appeared desirable to obtain the high-lift and lateral control characteristics for a wing utilized on one of the more representative configurations.

The wing selected and presented in this paper is the one utilized on the configuration referred to as configuration I in reference 4. The high-lift devices used on this wing are a single-slotted trailing-edge flap, a double-slotted trailing-edge flap, a spoiler-slot-deflector high-lift device, and a leading-edge flap. Spoiler-slot deflectors are used for lateral control in both the deflected and neutral positions of the trailing-edge flap.

The purpose of this paper is to present the results of this high-lift and lateral-control investigation made in the Langley 300-MPH 7- by 10-foot tunnel.

## SYMBOLS

The longitudinal characteristics are referred to the wind-axis system and the lateral control characteristics are referred to the body-axis system. Lift, drag, and pitching moments are nondimensionalized with respect to the geometric characteristics associated with the maximum sweep condition. Rolling and yawing moments are based on the area of the maximum sweep condition and the span of the wing for which the data are presented. The moment center as shown in figure 1(a) corresponds to 25 percent of the mean aerodynamic chord of the 75° sweep condition.

CONFIDENTIAL

- $C_L$  lift coefficient,  $\frac{\text{Twice semispan lift}}{qS}$
- $C_D$  drag coefficient,  $\frac{\text{Twice semispan drag}}{qS}$
- $C_m$  pitching-moment coefficient,  $\frac{\text{Twice semispan pitching moment}}{qS\bar{c}}$
- $C_l$  rolling-moment coefficient,  $\frac{\text{Semispan rolling moment}}{qSb}$
- $C_{l_p}$   $\frac{\partial C_l}{\partial \left(\frac{pb}{2V}\right)}$ , radians
- $C_n$  yawing-moment coefficient,  $\frac{\text{Semispan yawing moment}}{qSb}$
- $\Delta C_L$  incremental lift coefficient resulting from flap deflection
- $\Delta C_D$  incremental drag coefficient resulting from flap deflection
- $\Delta C_m$  incremental pitching-moment coefficient resulting from flap deflection
- $q$  dynamic pressure,  $\frac{\rho V^2}{2}$ , lb/sq ft
- $V$  velocity, ft/sec
- $\rho$  density, slugs/cu ft
- $S$  twice semispan wing area ( $75^\circ$  sweep condition), 12.548 sq ft
- $\bar{c}$  mean aerodynamic chord ( $75^\circ$  sweep condition), 2.9395 ft
- $c$  local chord, ft
- $c_f$  local flap chord, ft
- $b$  twice model semispan

L  
1  
5  
2  
7



$\alpha$	angle of attack, deg
$\Lambda$	wing leading-edge sweep angle, deg
$\delta_n$	leading-edge-flap deflection (positive leading edge up)
$\delta_f$	trailing-edge-flap deflection (positive trailing edge down)
$\delta_d$	deflector projections, fraction of wing chord
$\delta_s$	spoiler projections, fraction of wing chord
$\frac{pb}{2V}$	rolling effectiveness parameter, $\frac{\partial C_l}{\partial C_{l_p}}$ , radians

## MODEL

A drawing of the semispan variable-sweep wing is shown in figure 1(a). The pivot point for the outer wing panels was located at approximately 51 percent of the wing semispan in the 75° sweepback condition. The movable outer wing panel was tested at leading-edge sweep angles of 25°, 45°, 60°, and 75°. The inboard panel was fixed at  $\Lambda = 60^\circ$ . The wing aspect ratio varied from 5.148 for the 25° swept-back wing to 1.894 for the 75° sweptback wing. The fixed portion of the wing had NACA 63A004.5 airfoil sections parallel to the wing root chord line and the movable portion of the wing had NACA 63A006 airfoil sections parallel to the wing root chord line when the outer panel was swept 25°. A 1/8-inch-thick end plate 1 inch larger than the wing root was attached to the wing root to divert the airflow associated with leakage into the tunnel through the balance clearance hole.

Figure 1(b) shows a drawing of the wing in the 25° swept position with section views showing a leading-edge flap, a single-slotted trailing-edge flap, and a double-slotted trailing-edge flap in both the flaps-neutral and flaps-deflected positions. The leading-edge flap extends the length of the movable outer panel and has its hinge line along the 15-percent wing chord line.

The single-slotted flap has a chord equal to 25 percent of the wing chord and when deflected has its hinge line at the 80-percent wing chord line. The main flap of the double-slotted-flap configuration has a chord equal to 25 percent of the wing chord and a vane with a chord



equal to 50 percent of the flap chord. The double-slotted flap was extended and then deflected as a unit with the hinge line at the 80-percent wing chord line.

Figure 1(c) shows the details of the gaps (expressed as fractions of the wing chord) for the single-slotted flap and the double-slotted flap. The ordinates for the flap used as a single- or double-slotted flap are listed in table I and the ordinates for the vane used with the flap to make a double-slotted flap are listed in table II.

Figure 1(d) is a drawing of the wing in the 25° sweep position with section views showing the spoiler-slot-deflector high-lift and lateral control device in both the neutral and deflected positions. The single-slotted-flap portion extends from 0.172b/2 to 0.388b/2 and the spoiler-slot-deflector high-lift device extends from 0.388b/2 to the wing tip. The spoiler-slot-deflector high-lift device is a combination lateral control and high-lift device. For the high-lift condition, the spoiler is undeflected, thereby providing the same gap as shown in figure 1(c) for the single-slotted flap. The deflector is projected to form a scoop on the under side of the wing to allow air to flow through the slot and produce lift in the same way as a single-slotted flap. In order to obtain lateral control in the trailing-edge-flap-deflected condition the spoiler or the spoiler and deflector can be projected from this neutral position (ref. 5). In the flap-neutral condition the spoiler slot deflector provides lateral control in the same way as a conventional spoiler slot deflector. The spoiler and deflector were made of 0.0625-inch steel plate with chords equal to 15 and 10 percent of the wing chord, respectively. The spoiler was hinged about the 65-percent wing chord line and the deflector was hinged about the leading edge of the flap (75-percent wing chord line when the flap is undeflected). Over the span of the spoiler and deflector there was a slot through the wing between the 65- and 75-percent wing chord lines except for three 0.5-inch-wide stiffener webs whose center lines were at the 59-, 78-, and 99-percent semispan stations of the wing in the 25° sweep position. The accompanying trailing-edge flap has a chord equal to 25 percent of the wing chord with its hinge line at the 80-percent wing chord line.

Figure 1(e) is a drawing of the wing in the 25° and 75° sweep conditions with section views showing a spoiler-slot deflector in the neutral and projected positions. This spoiler-slot deflector is dimensionally identical to the aforementioned one.

#### TEST AND CORRECTIONS

The investigation was made in the Langley 300-MPH 7- by 10-foot tunnel at a dynamic pressure of 25.20 lb/sq ft which corresponds to a

Reynolds number of  $2.65 \times 10^6$  based on the mean aerodynamic chord of the wing in the  $75^\circ$  sweep condition. The model was instrumented with a five-component strain-gage balance and mounted  $3/16$  inch from the wall of the wind tunnel. The forces and moments were measured through an angle-of-attack range that varied from  $-4^\circ$  to about  $25^\circ$ . Transition strips  $1/8$  inch wide of No. 80 carborundum grit were placed at the 5-percent chord of the wing upper and lower surfaces.

Blockage corrections were determined by the method of reference 6 and were applied to the dynamic pressure. Jet boundary corrections applied to the angle of attack and drag were calculated with the aid of reference 7. Inasmuch as the spoiler-induced load is considerably more localized spanwise than it is for flap-type controls (ref. 8) no reflection plane corrections have been applied to the semispan data.

#### PRESENTATION OF DATA

The data for the semispan variable-sweep-wing configuration are presented in the following order:

	Figure
Effect of wing leading-edge sweep angle on the longitudinal aerodynamic characteristics. $\delta_n = 0^\circ$ ; $\delta_f = 0^\circ$ . . . . .	2
Effect of deflection of a leading-edge flap on the longitudinal aerodynamic characteristics. $\delta_f = 0^\circ$ ; $\Lambda = 25^\circ$ . . . . .	3
Effect of deflections of a single-slotted flap on the longitudinal aerodynamic characteristics for several leading-edge-flap deflections. $\Lambda = 25^\circ$ . . . . .	4
Effect of deflections of a double-slotted flap on the longitudinal aerodynamic characteristics for several leading-edge-flap deflections. $\Lambda = 25^\circ$ . . . . .	5
Effect of deflections of a spoiler-slot-deflector high-lift device on the longitudinal aerodynamic characteristics for several leading-edge flap deflections. $\Lambda = 25^\circ$ ; $\delta_s = 0$ ; $\delta_d = 0.02$ . . . . .	6
Effect of deflections of three types of trailing-edge flaps on the longitudinal aerodynamic characteristics for typical take-off conditions. $\Lambda = 25^\circ$ ; $\delta_n = -20^\circ$ . . . . .	7
Effect of deflections of three types of trailing-edge flaps on the longitudinal aerodynamic characteristics for typical landing conditions. $\Lambda = 25^\circ$ ; $\delta_n = -20^\circ$ . . . . .	8
Effect of spoiler projections on the aerodynamic characteristics for various lateral control projections. $\Lambda = 25^\circ$ ; $\delta_d = 0.02$ ; $\delta_n = -20^\circ$ ; $\delta_f = 35^\circ$ . . . . .	9

Figure

Effect of spoiler projections on the aerodynamic characteristics for various lateral control projections.  $\Lambda = 25^\circ$ ;  $\delta_d = 0.02$ ;  $\delta_n = -20^\circ$ ;  $\delta_f = 45^\circ$  . . . . . 10

Effect of spoiler and deflector projections on the aerodynamic characteristics for various lateral control projections.  $\Lambda = 25^\circ$ ;  $\delta_n = 0^\circ$ ;  $\delta_f = 0^\circ$  . . . . . 11

Effect of spoiler and deflector projections on the aerodynamic characteristics for various lateral control projections.  $\Lambda = 75^\circ$ ;  $\delta_n = 0^\circ$ ;  $\delta_f = 0^\circ$  . . . . . 12

RESULTS

Longitudinal Aerodynamic Characteristics

A comparison of the longitudinal aerodynamic characteristics of the three trailing-edge flaps for several leading-edge-flap deflection angles (figs. 4 to 6) indicates that for the  $25^\circ$  sweep condition there is a nearly linear increase in lift coefficient with increasing trailing-edge-flap deflection up to approximately  $30^\circ$  deflection for the single-slotted flap (fig. 4) and for the spoiler-slot-deflector high-lift device (fig. 6) and to approximately  $40^\circ$  for the double-slotted flap (fig. 5). Further increases in flap deflection resulted in only small increases in lift effectiveness and were accompanied by rather large increases in drag indicating separation of the flow on the flap.

It should be noted that for the wing with trailing-edge flaps deflected there occurs a rather abrupt unstable variation of pitching moment with lift at moderate lift coefficients. As the deflection of the leading-edge flap is increased negatively, however, this unstable variation in pitching moment is progressively delayed to higher lift coefficients.

Incremental variations in the lift, drag, and pitching-moment coefficients for the three types of trailing-edge-flap devices with the leading-edge flap deflected to  $-20^\circ$  are presented in figure 7 for a take-off condition and in figure 8 for a landing condition. The trailing-edge-flap deflection angles for the take-off condition were chosen from consideration of both the lift developed and the lift-to-drag ratio, whereas, for the landing condition only maximum lift capabilities were considered. Above the take-off flap deflection angles slight increases in lift resulted with an accompanying large increase in drag. The data of figures 7 and 8 show that for the chosen flap deflection angles the double-slotted flap resulted in the largest increment in lift, drag,



L  
1  
5  
2  
7

and pitching-moment coefficients throughout the test angle-of-attack range. Deflections of the single-slotted flap and the spoiler-slot-deflector high-lift device resulted in approximately the same increment in lift, drag, and pitching-moment coefficients except at the lower flap deflection angle (fig. 7) where large differences occurred in the incremental lift and drag at the higher angles of attack. It is felt that if the optimum deflector projection had been used these differences which occurred at the lower flap deflection angle would not have been present.

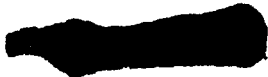
The spoiler-slot-deflector high-lift device is, of course, a lateral control device as well as a high-lift device. The effects of spoiler-slot-deflector projection when used as a lateral control on the longitudinal characteristics are presented in figures 9(a), 10(a), 11(a), and 12(a). These data on the longitudinal characteristics show that increasing the spoiler-slot-deflector projections decreased the lift coefficient, increased the drag coefficient, and produced a positive increment of pitching-moment coefficient with no appreciable change in the slope of the pitching-moment curves.

#### Lateral Control Characteristics

The lateral control characteristics of the spoiler-slot-deflector high-lift device with flap deflected on the  $25^\circ$  sweptback wing, and the flap neutral on the  $25^\circ$  and  $75^\circ$  sweptback wing are presented as the variation of rolling- and yawing-moment coefficients with angle of attack in figures 9(b), 10(b), 11(b), and 12(b). These data show that the rolling-moment effectiveness increases with increasing spoiler-slot-deflector projections for all configurations tested. For the higher spoiler-slot-deflector projections adequate rolling moment and favorable yawing moment are produced throughout the usable angle-of-attack range. With regard to the roll power in the flaps-neutral condition estimates of the damping in roll indicate that a value of  $pb/2V$  of 0.06 can be developed for angles of attack up to about  $16^\circ$  with 10-percent spoiler and 7.5-percent deflector projections.

#### CONCLUDING REMARKS

An investigation was made to determine the effect of leading-edge and trailing-edge-flap deflections and spoiler-slot-deflector projections on the high-lift and lateral control characteristics of a semispan variable-sweep-wing configuration. The deflections of the leading-edge and trailing-edge flap and the projections of the spoiler-slot deflector indicated the following effects.



Nearly linear increases in lift coefficient were obtained with increasing flap deflection up to approximately  $30^\circ$  deflection for the single-slotted flap and the spoiler-slot-deflector configuration and to approximately  $40^\circ$  for the double-slotted flap. Further increases in flap deflection resulted in only small increases in lift effectiveness and were accompanied by rather large increases in drag.

Rather abrupt unstable variation of pitching moment with lift occurred at moderate lift coefficients for the wing with trailing-edge flaps deflected. Increasing the deflection of the leading-edge flap progressively delayed this unstable variation to higher lift coefficients.

Increasing the spoiler-slot-deflector projections when used as a lateral control device decreased the lift coefficient, increased the drag coefficient, and produced a positive increment of pitching-moment coefficient with no appreciable change in the slope of the pitching-moment curves.

Adequate rolling moment and favorable yawing moment are produced by the higher spoiler-slot-deflector projections throughout the usable angle-of-attack range.

Langley Research Center,  
National Aeronautics and Space Administration,  
Langley Field, Va., March 31, 1961.



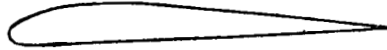
CONFIDENTIAL

## REFERENCES

1. Alford, William J., Jr., and Henderson, William P.: An Exploratory Investigation of the Low-Speed Aerodynamic Characteristics of Variable-Wing-Sweep Airplane Configurations. NASA TM X-142, 1959.
2. Alford, William J., Jr., Luoma, Arvo A., and Henderson, William P.: Wind-Tunnel Studies at Subsonic and Transonic Speeds of a Multiple-Mission Variable-Wing-Sweep Airplane Configuration. NASA TM X-206, 1959.
3. Polhamus, Edward C., and Hammond, Alexander D.: Aerodynamic Research Relative to Variable-Sweep Multimission Aircraft. Ch. II of Compilation of Papers Summarizing Some Recent NASA Research on Manned Military Aircraft. NASA TM X-420, 1960, pp. 13-38.
4. Spencer, Bernard, Jr.: Stability and Control Characteristics at Low Subsonic Speeds of an Airplane Configuration Having Two Types of Variable-Sweep Wings. NASA TM X-303, 1960.
5. Hammond, Alexander D., and Huffman, Jarrett K.: A Low-Speed Investigation of a High-Lift Lateral-Control Device Consisting of a Spoiler-Slot-Deflector and a Trailing-Edge Flap on a Tapered 45° Sweptback Wing. NACA RM L56H31, 1956.
6. Herriot, John G.: Blockage Corrections for Three-Dimensional-Flow Closed-Throat Wind Tunnels, With Consideration of the Effect of Compressibility. NACA Rep. 995, 1950. (Supersedes NACA RM A7B28.)
7. Polhamus, Edward C.: Jet-Boundary-Induced-Upwash Velocities for Swept Reflection-Plane Models Mounted Vertically in 7- by 10-Foot, Closed, Rectangular Wind Tunnels. NACA TN 1752, 1948.
8. Hammond, Alexander D.: Loads on Wings Due to Spoilers at Subsonic and Transonic Speeds. NACA RM L55E17a, 1955.



TABLE I.- TRAILING-EDGE-FLAP ORDINATES



L  
1  
5  
2  
7

Station	Ordinate, percent chord	
	Upper	Lower
0	-4.20	-4.20
1.24	-2.41	-5.31
2.52	-1.54	-5.70
5.00	-0.34	-5.82
7.52	0.72	-5.78
10.00	1.66	-5.77
15.00	2.97	-5.46
20.00	3.73	-5.14
30.00	4.50	-4.50
40.00	3.87	-3.87
60.00	2.60	-2.60
80.00	1.32	-1.32
100.00	.05	-.05



0317120A.1030

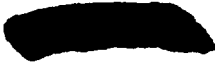


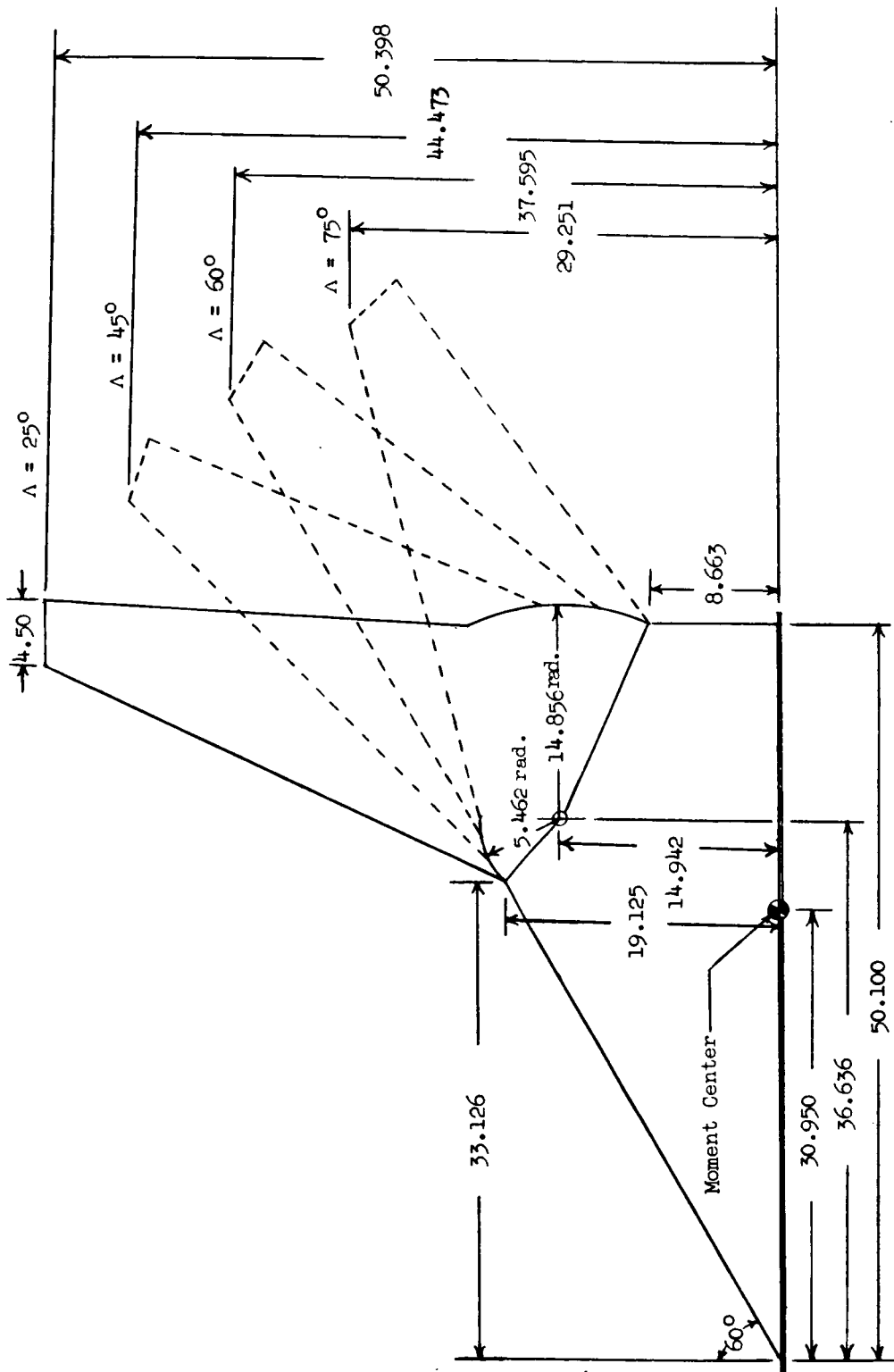
TABLE II.- VANE ORDINATES



L  
1  
5  
2  
7

Station	Ordinate, percent chord	Station	Ordinate, percent chord
	Upper		Lower
0	-19.13	0	-19.13
.74	-17.27	.16	-23.38
2.44	-14.19	2.39	-25.61
4.36	-11.62	3.93	-25.85
6.37	- 9.37	6.64	-25.64
10.52	- 5.27	9.24	-25.11
14.87	- 1.75	11.79	-24.22
24.22	3.78	16.68	-22.01
34.10	7.73	21.24	-19.11
44.29	10.75	30.59	-13.88
54.54	12.79	40.10	- 8.75
65.75	13.72	50.72	- 3.43
77.01	13.96	61.18	1.41
88.37	13.79	71.22	5.24
94.05	13.71	81.04	8.67
100.00	12.94	90.65	11.09
		95.33	12.18
		100.00	12.94

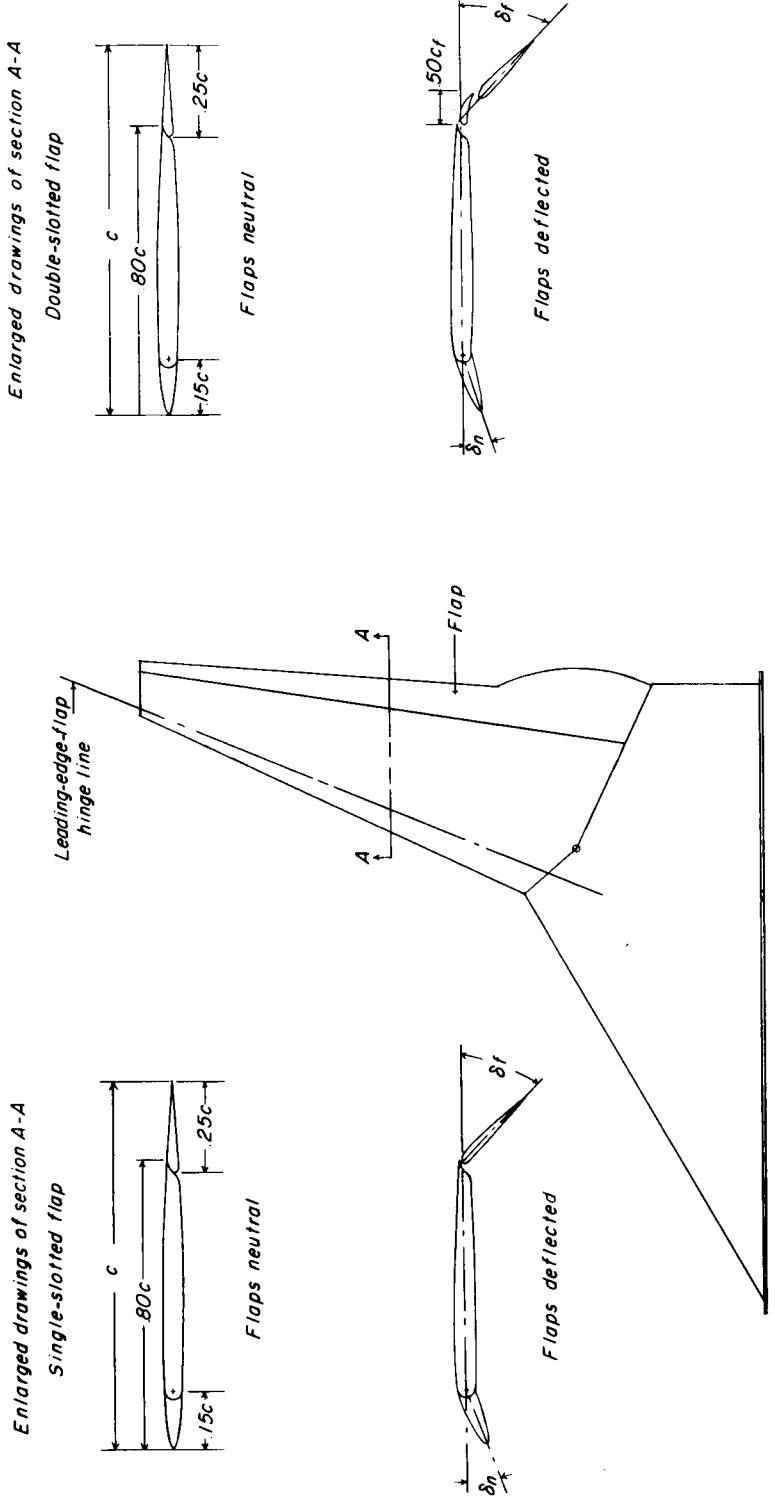




(a) Details of model.

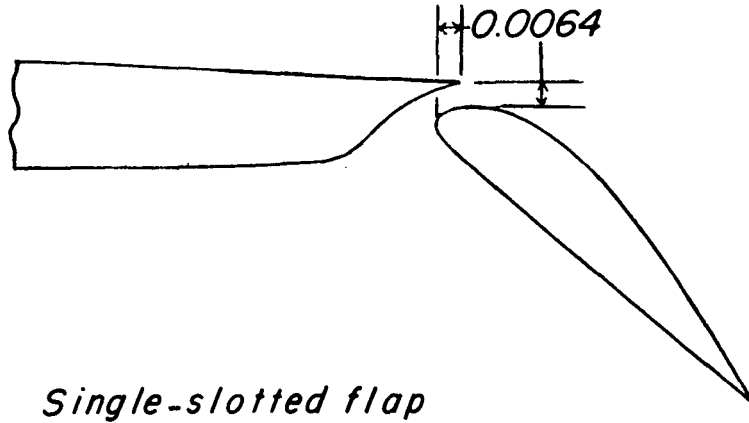
Figure 1.- Semispan variable-sweep-wing configuration. All dimensions are in inches.

I-1527

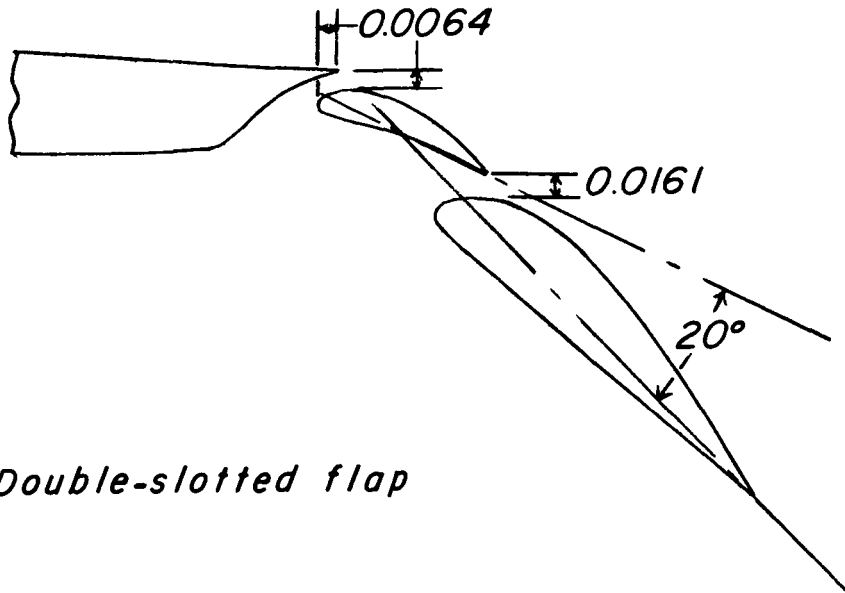


(b) Details of single-slotted and double-slotted flap configuration.

Figure 1.- Continued.



*Single-slotted flap*



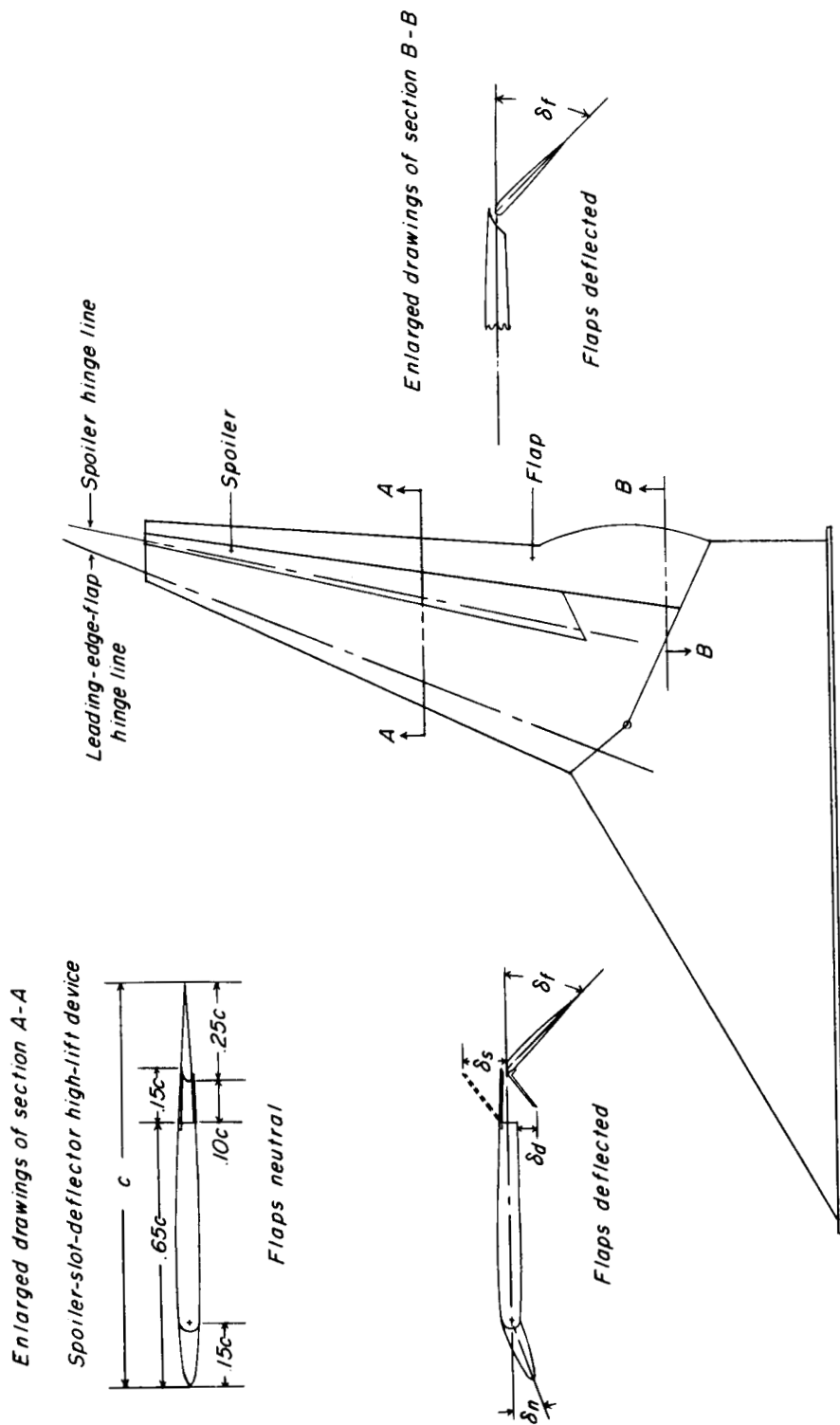
*Double-slotted flap*

(c) Details of gap size (expressed as fraction of wing chord) on the single-slotted and double-slotted flaps.

Figure 1.- Continued.



L-1527

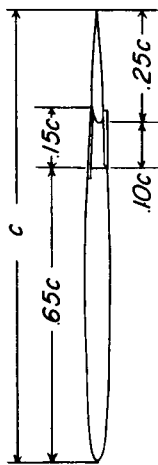


(d) Details of spoiler-slot-deflector high-lift and lateral control configuration.

Figure 1.- Continued.

I-1527

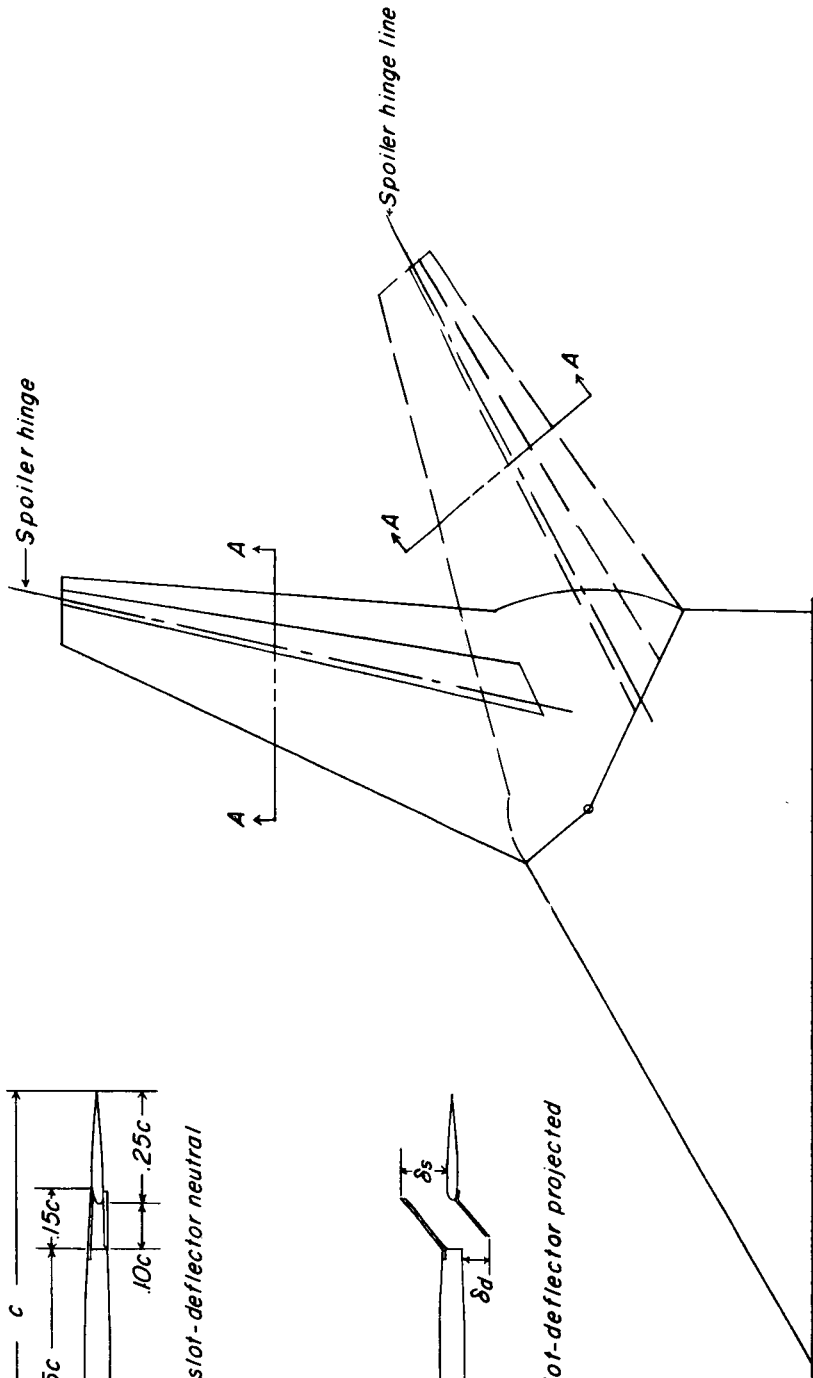
Enlarged drawings of section A-A  
Spoiler-slot-deflector lateral control devices



Spoiler-slot-deflector neutral



Spoiler-slot-deflector projected



(e) Details of spoiler-slot-deflector configuration.

Figure 1.- Concluded.

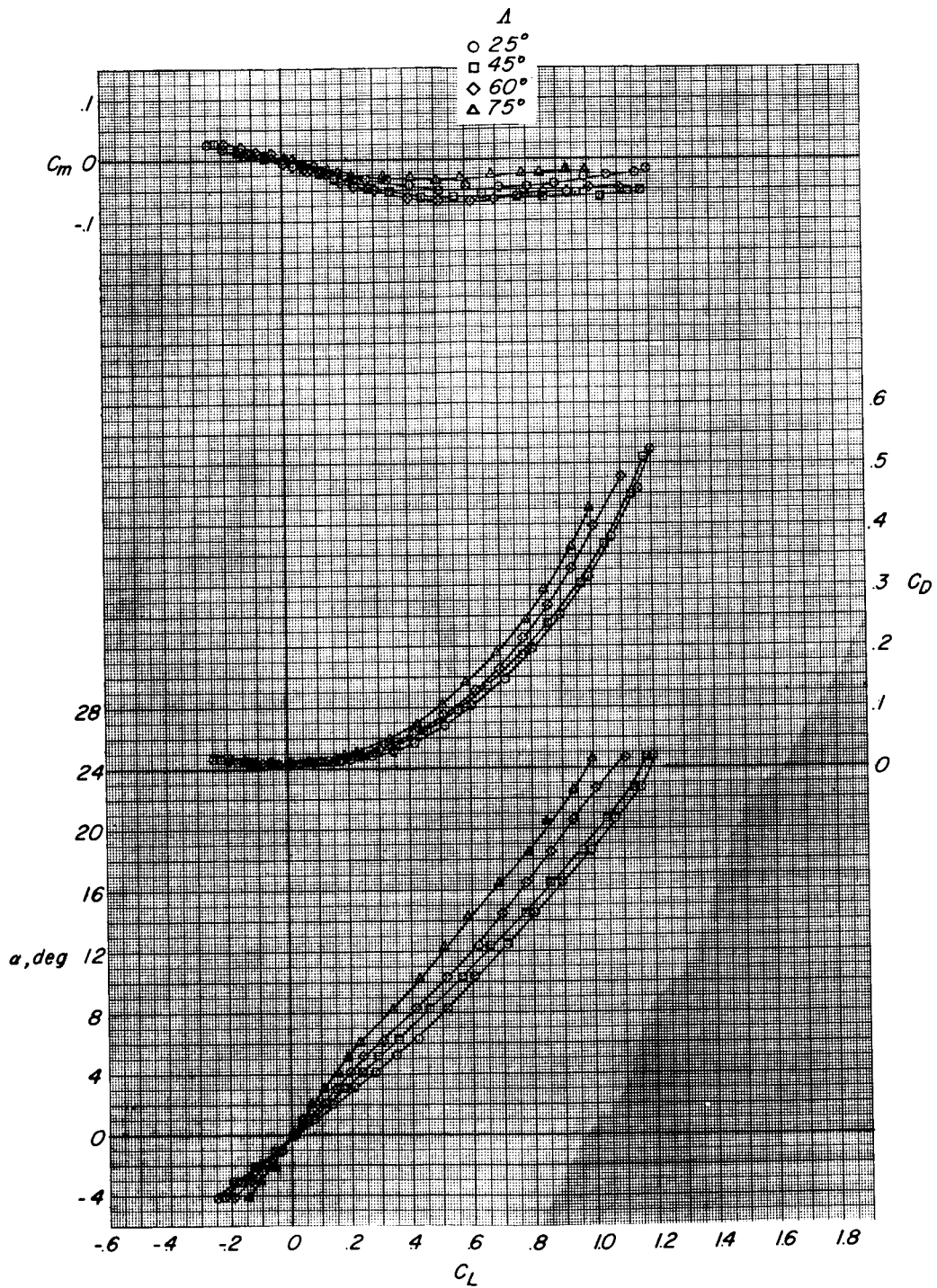


Figure 2.- Effect of wing leading-edge sweep angle on the longitudinal aerodynamic characteristics.  $\delta_n = 0^\circ$ ;  $\delta_f = 0^\circ$ .

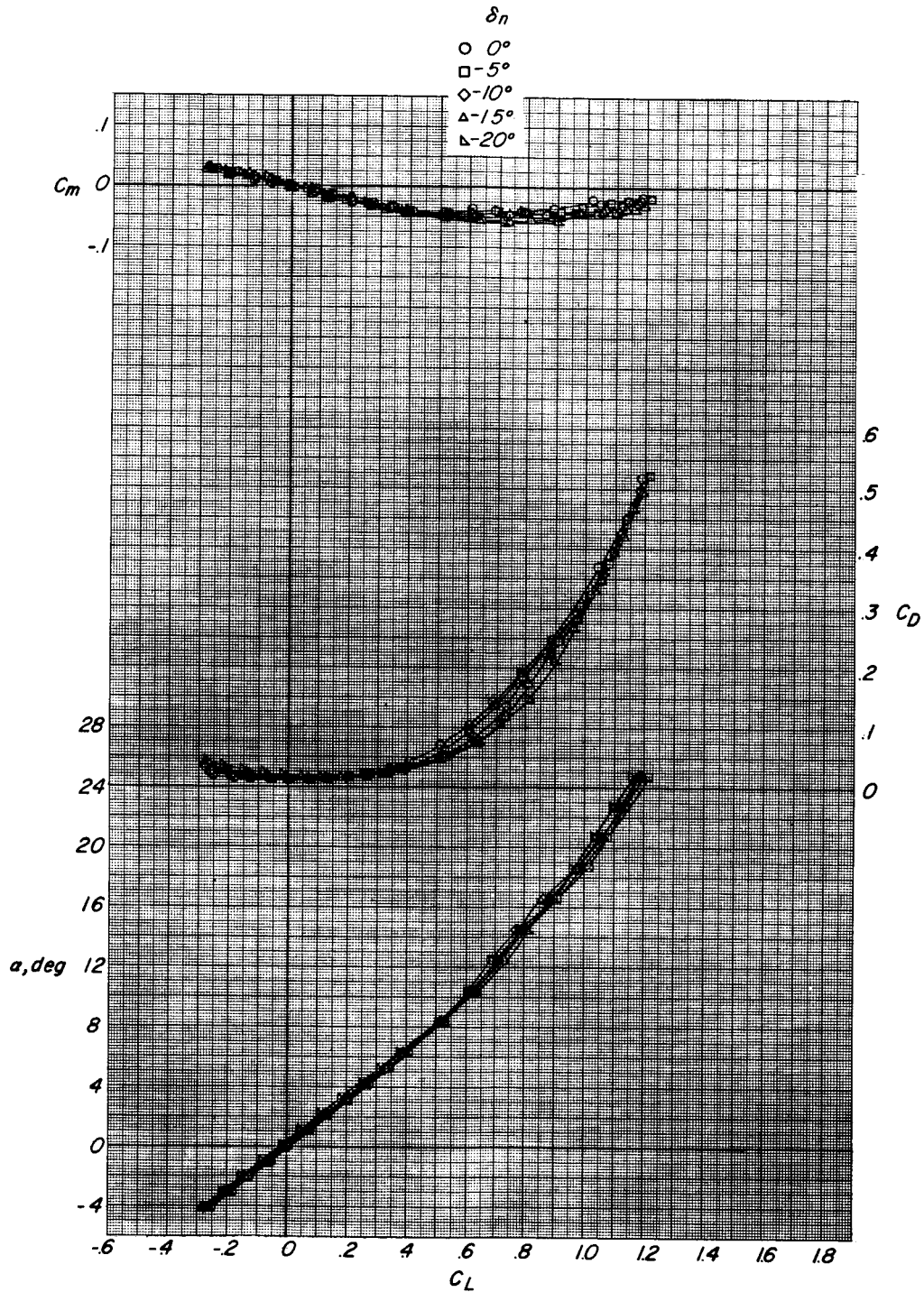
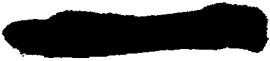
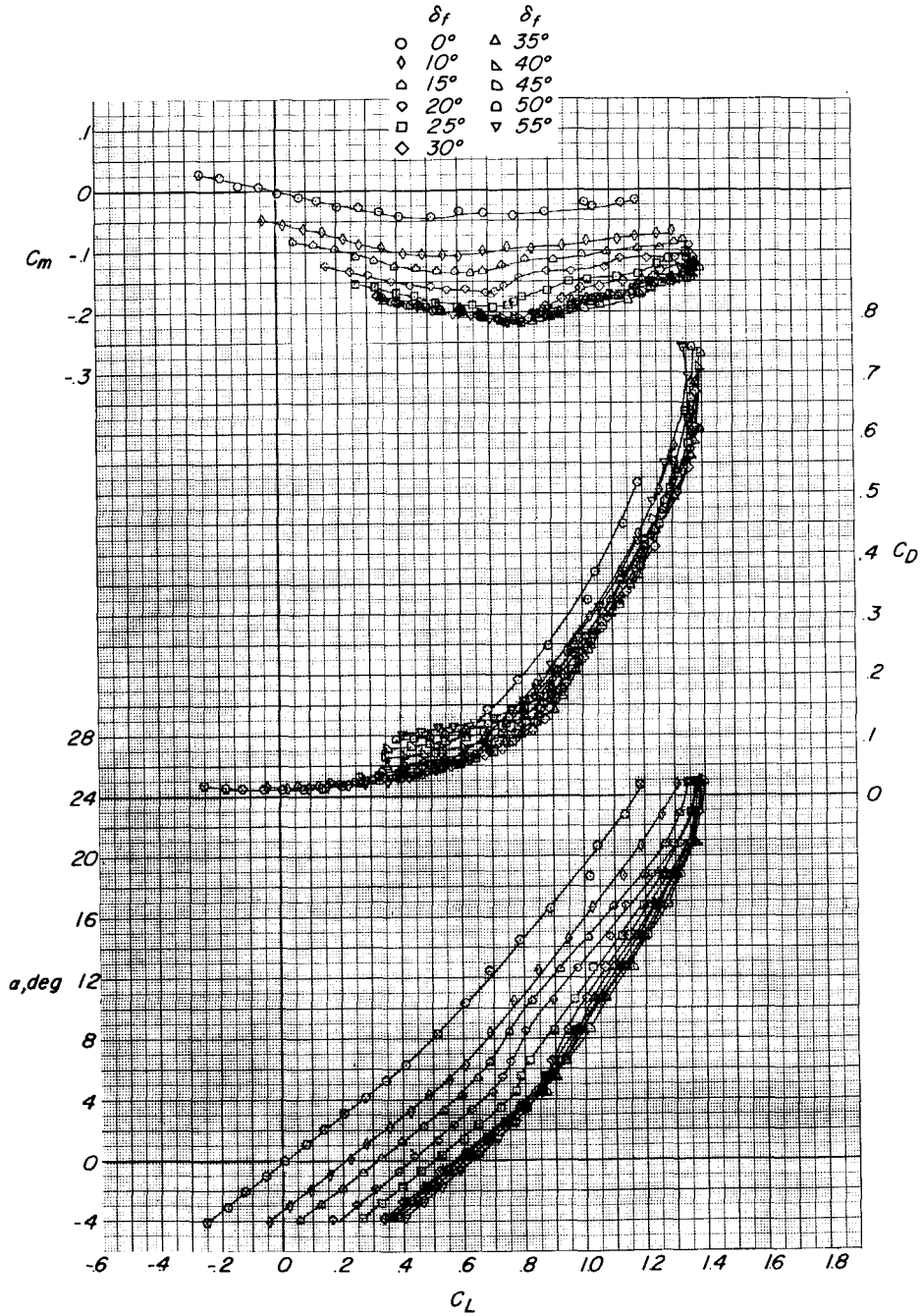


Figure 3.- Effect of deflections of a leading-edge flap on the longitudinal aerodynamic characteristics.  $\Lambda = 25^\circ$ ;  $\delta_f = 0^\circ$ .

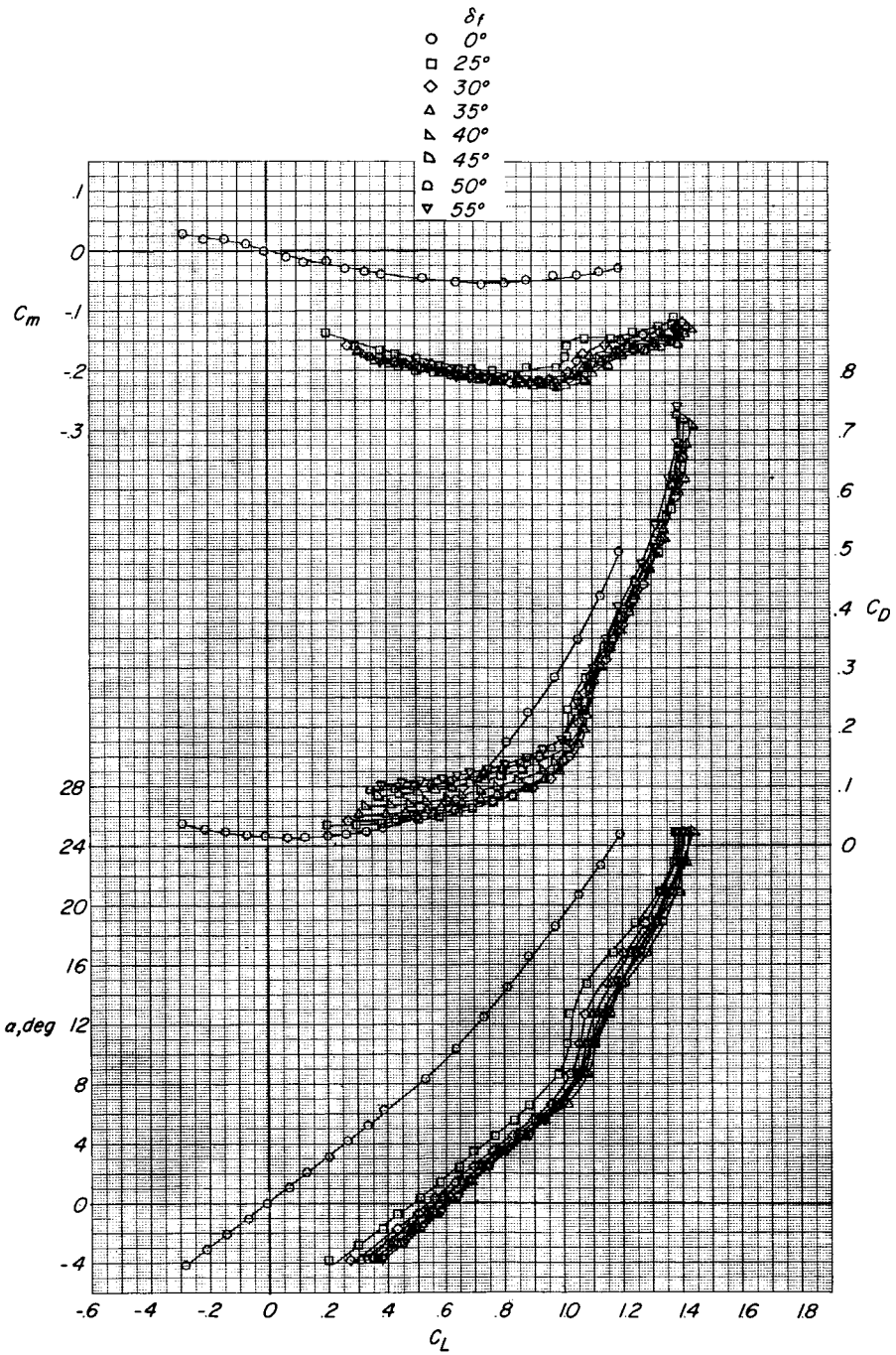




(a)  $\delta_n = 0^\circ$ .

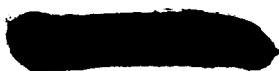
Figure 4.- Effect of deflection of a single-slotted flap on the longitudinal aerodynamic characteristics for several leading-edge-flap deflections.  $\Lambda = 25^\circ$ .

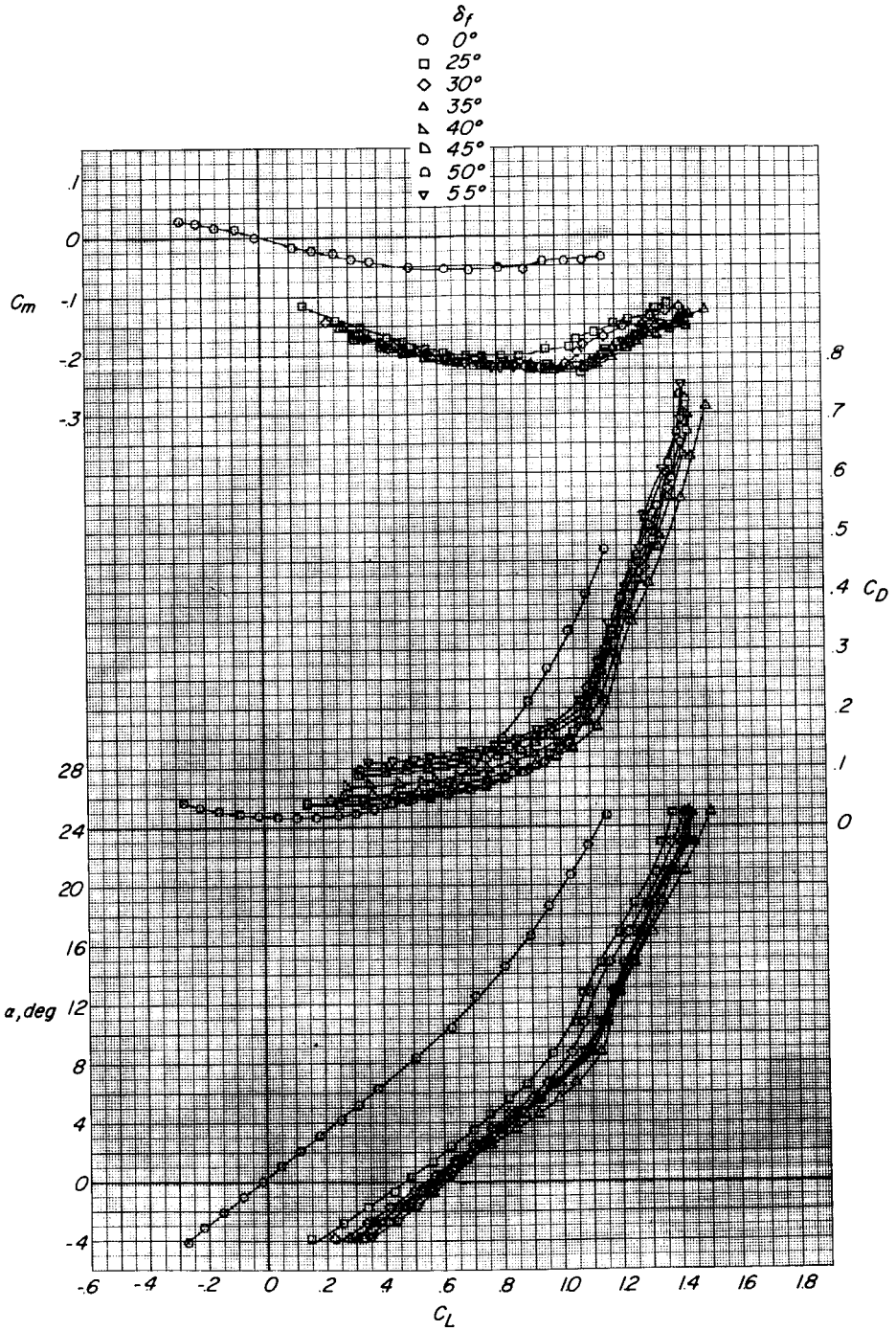
L-1527



(b)  $\delta_n = -15^\circ$ .

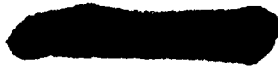
Figure 4.- Continued.

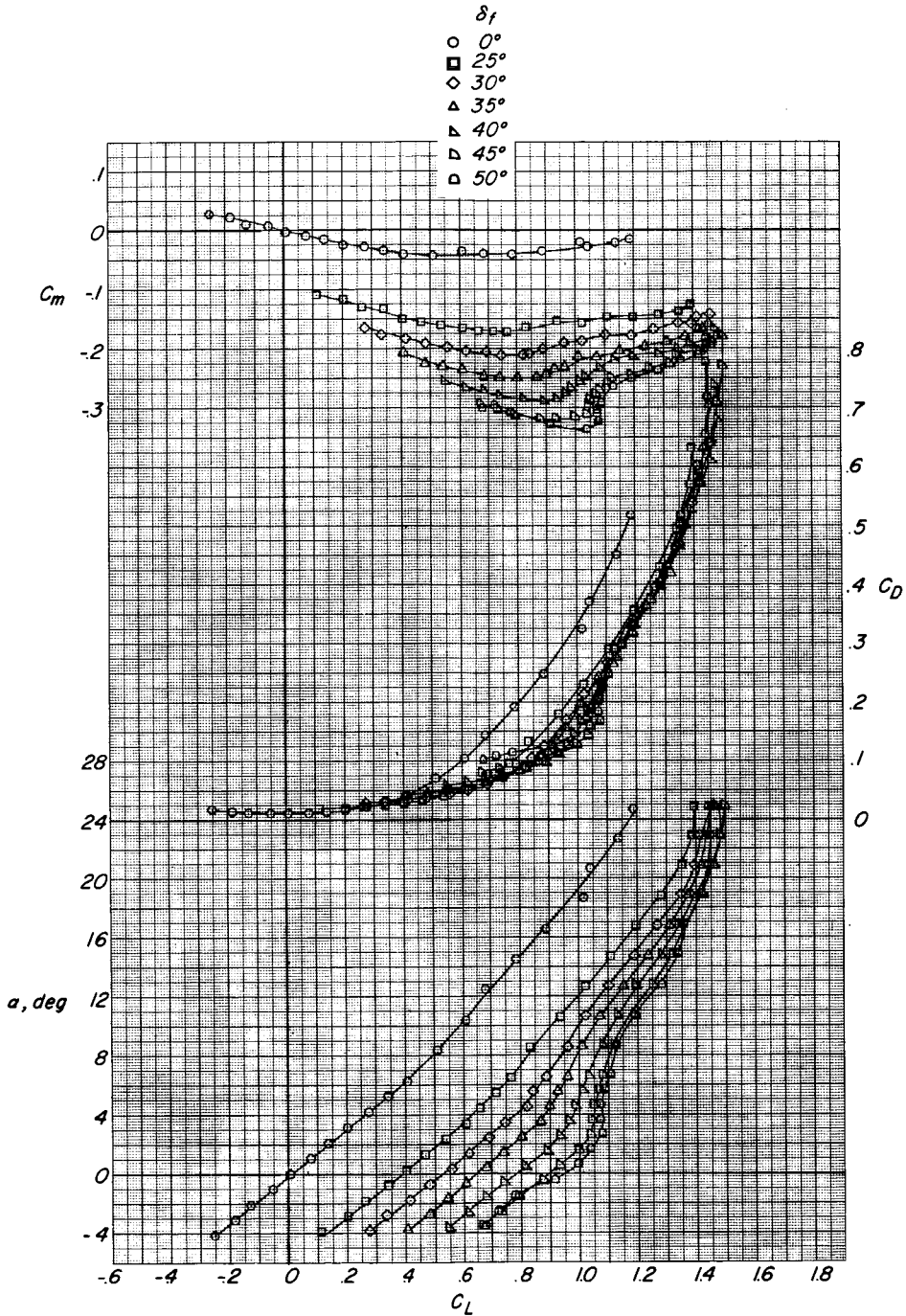




(c)  $\delta_n = -20^\circ$ .

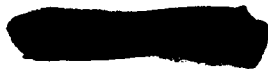
Figure 4.- Concluded.



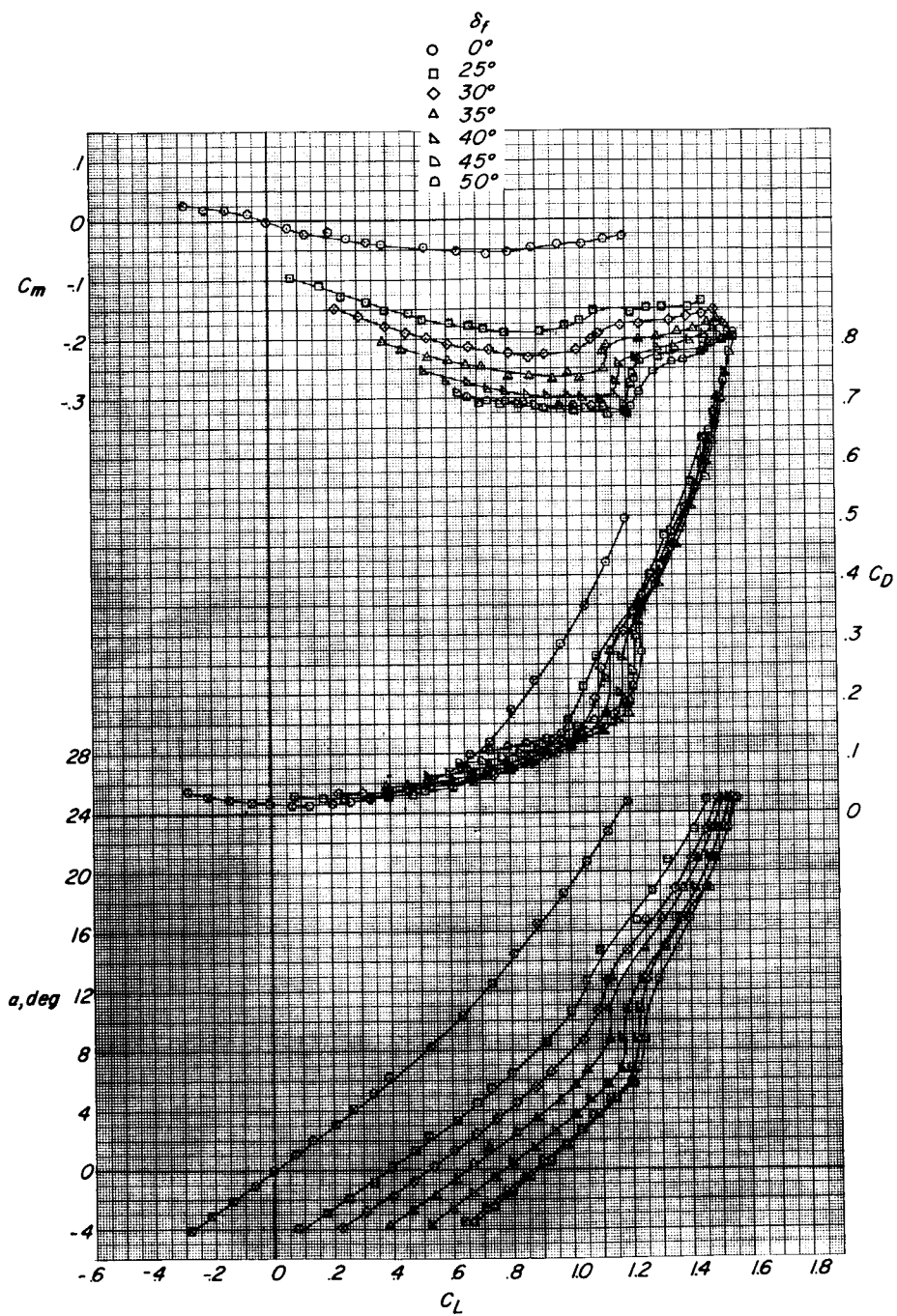


(a)  $\delta_n = 0^\circ$ .

Figure 5.- Effect of deflections of a double-slotted flap on the longitudinal aerodynamic characteristics for several leading-edge-flap deflections.  $\Lambda = 25^\circ$ .

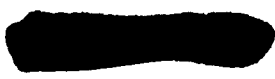


L-1527

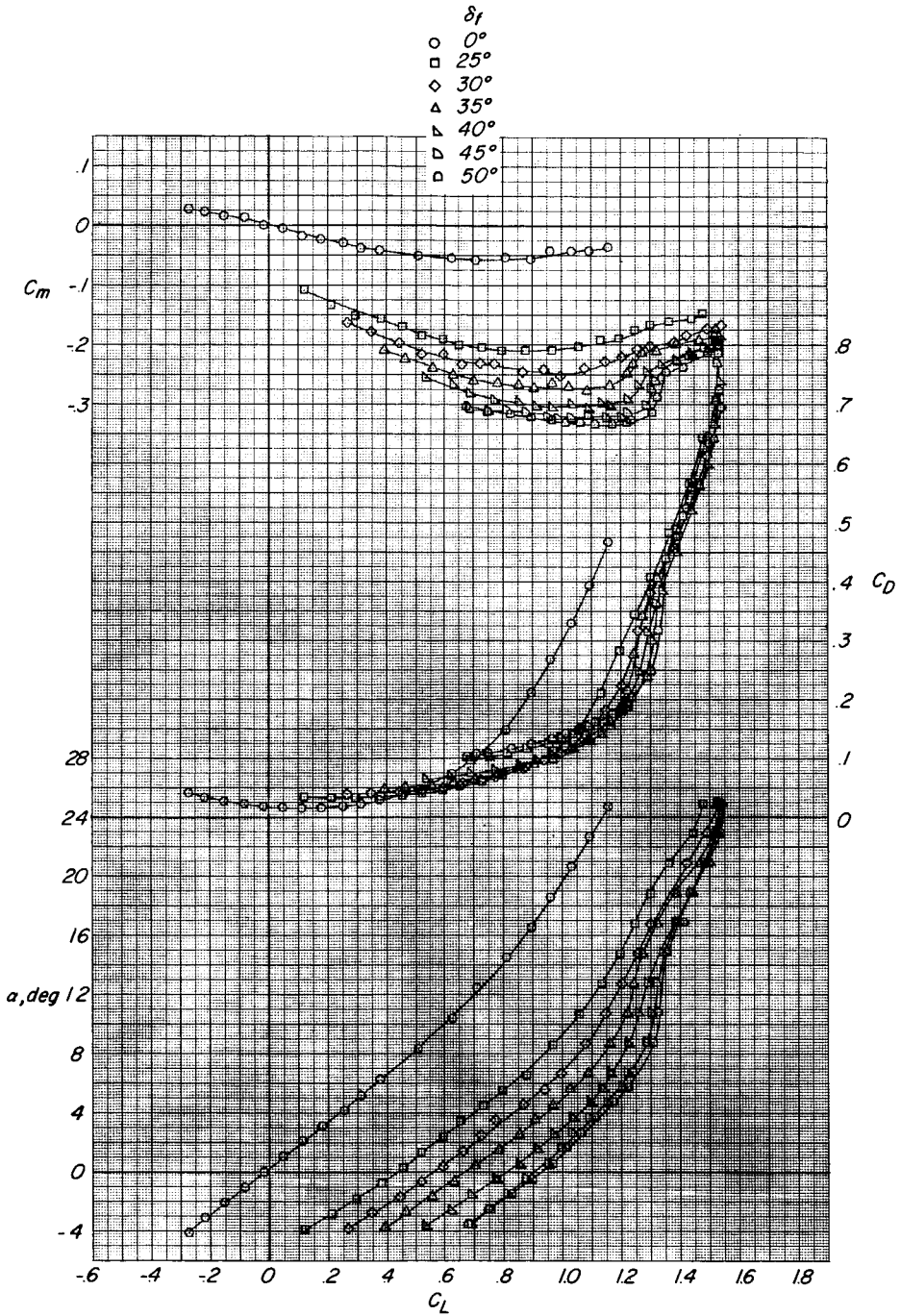


(b)  $\delta_n = -15^\circ$ .

Figure 5.- Continued.



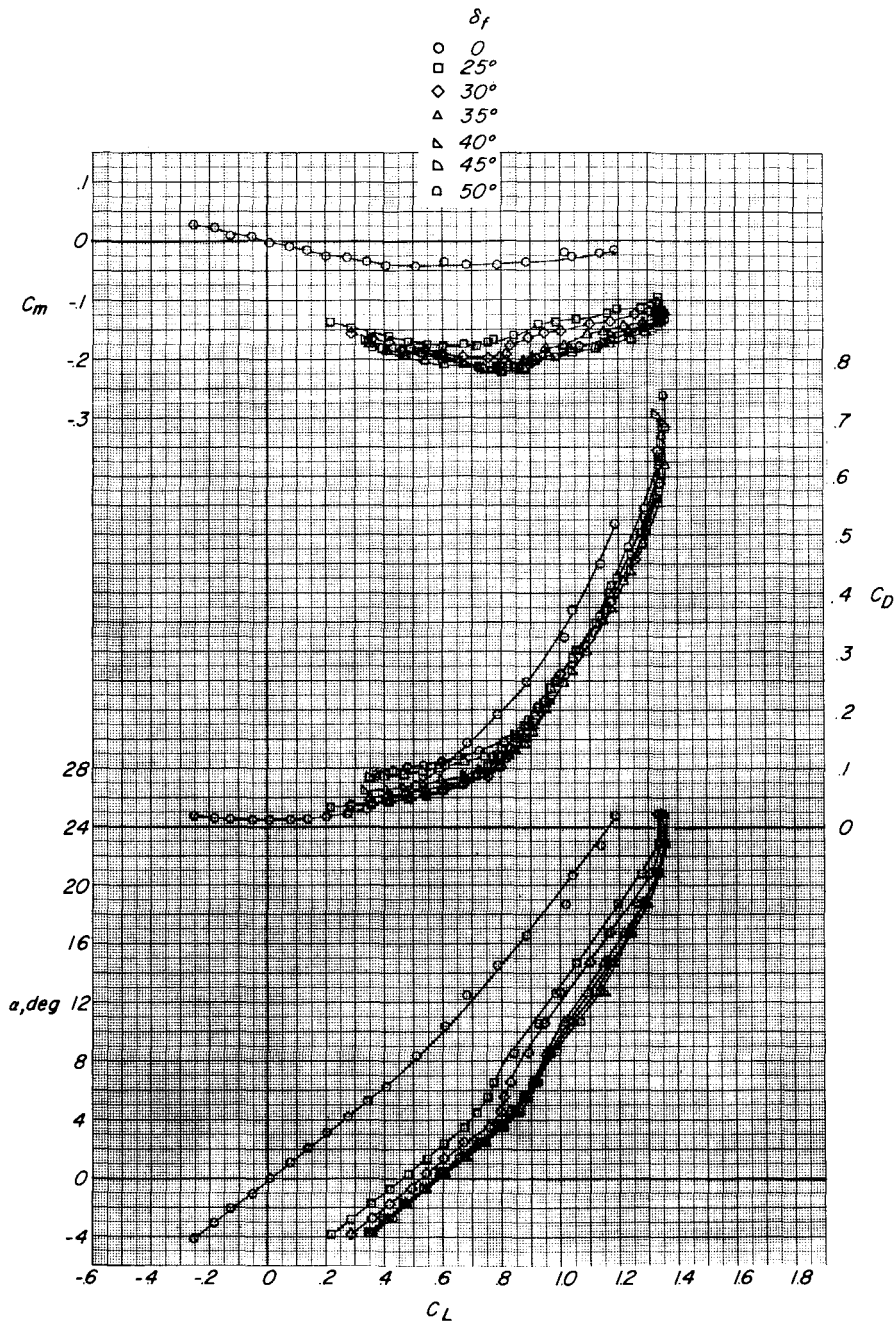
L-1527



(c)  $\delta_n = -20^\circ$ .

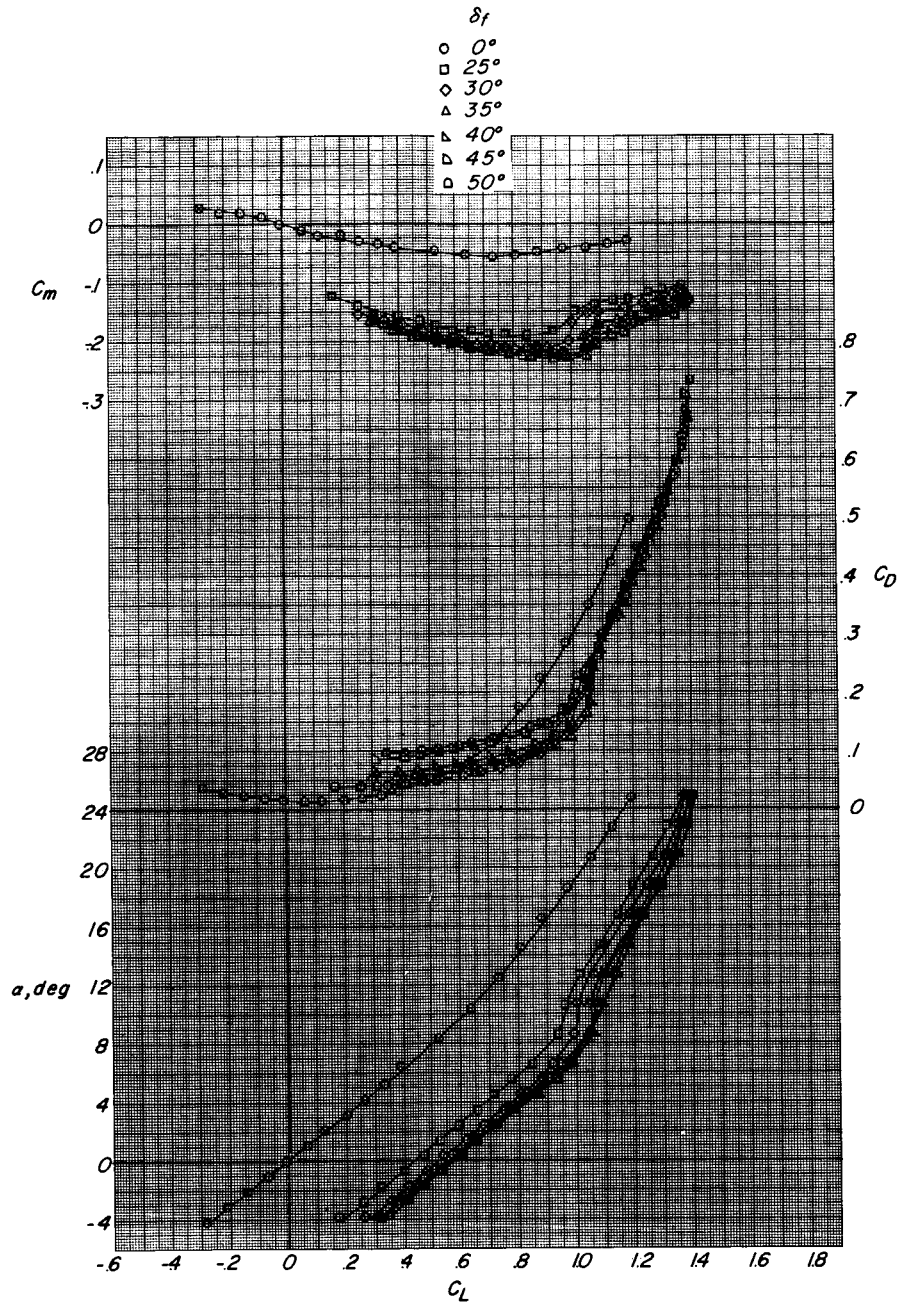
Figure 5.- Concluded.





(a)  $\delta_n = 0^\circ$ .

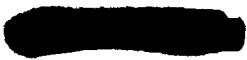
Figure 6.- Effect of deflections of a spoiler-slot-deflector high-lift device on the longitudinal aerodynamic characteristics for several leading-edge-flap deflections.  $\Lambda = 25^\circ$ ;  $\delta_s = 0$ ;  $\delta_d = 0.02$ .

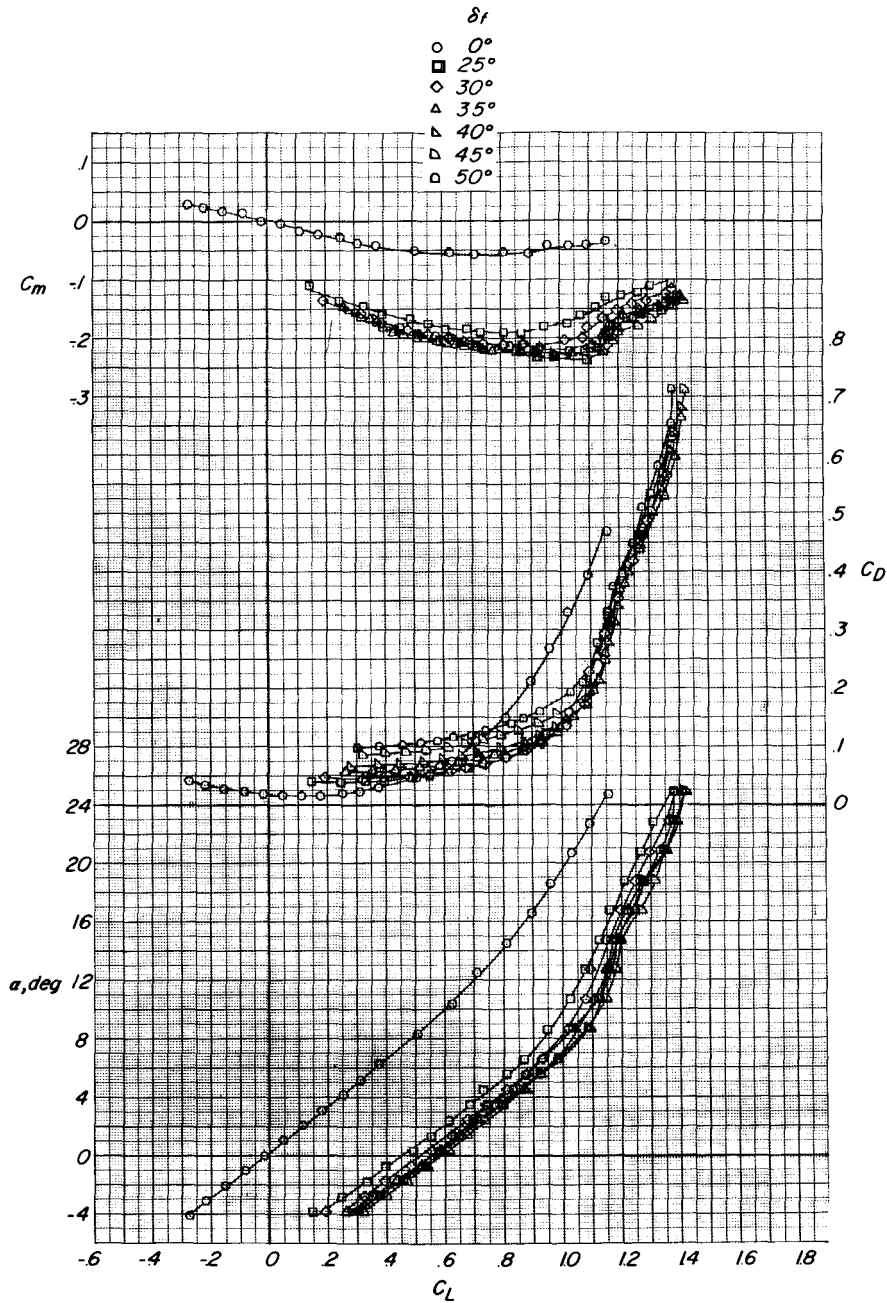


(b)  $\delta_n = -15^\circ$ .

Figure 6.- Continued.

I-1527

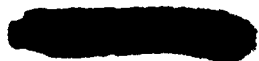




I-1527

(c)  $\delta_n = -20^\circ$ .

Figure 6.- Concluded.



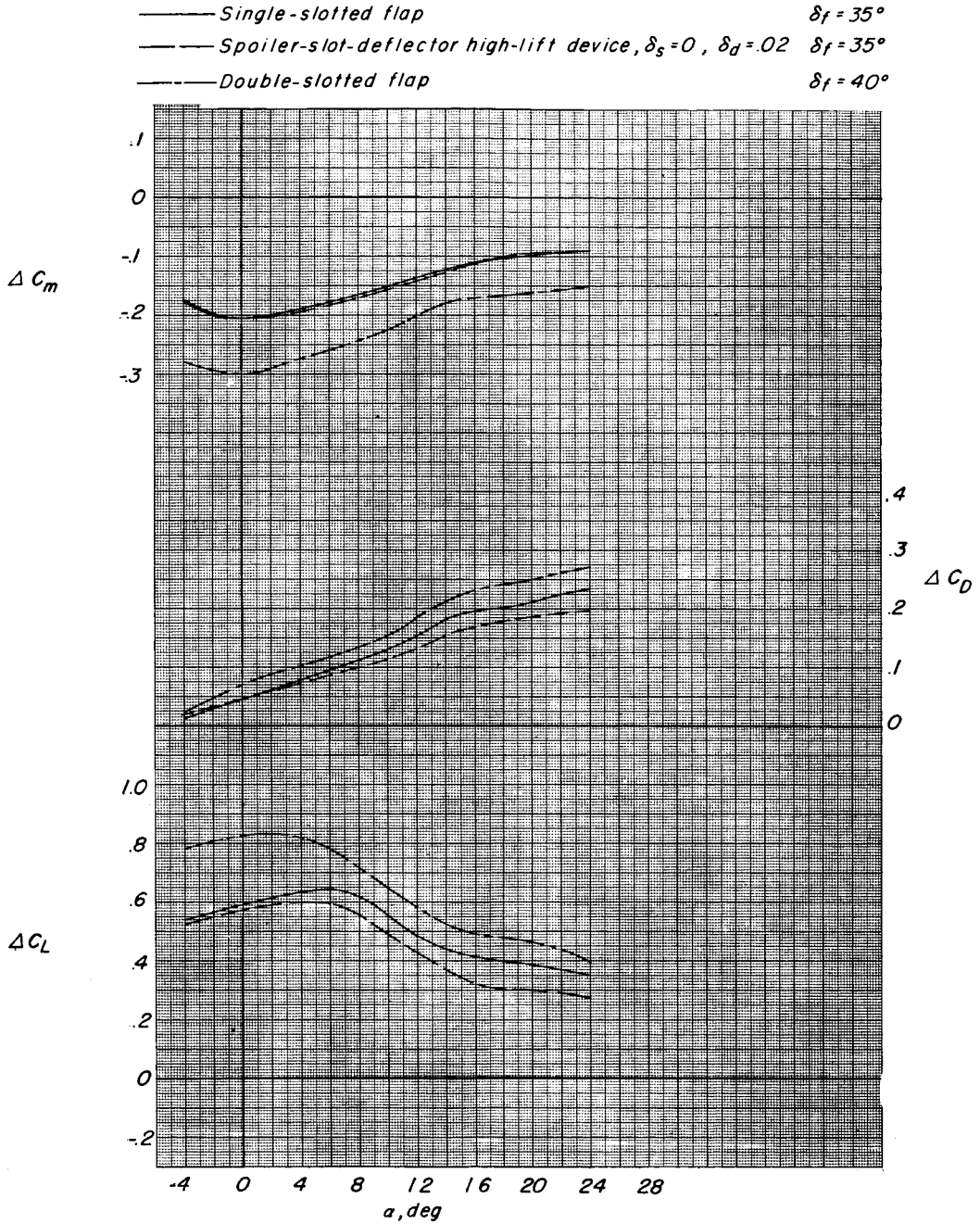


Figure 7.- Effect of deflections of three types of trailing-edge flaps on the longitudinal aerodynamic characteristics for typical take-off conditions.  $\Lambda = 25^\circ$ ;  $\delta_n = -20^\circ$ .

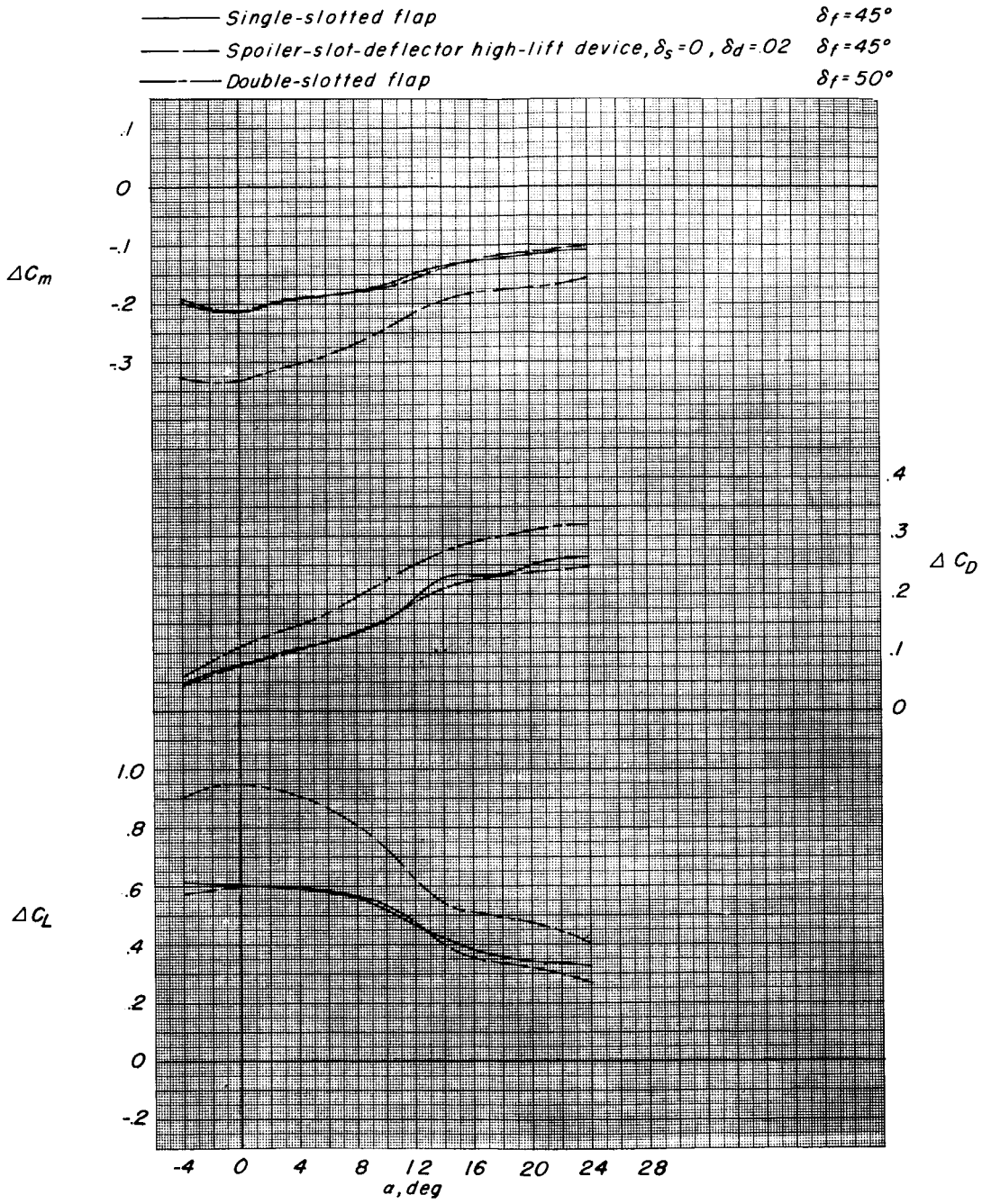
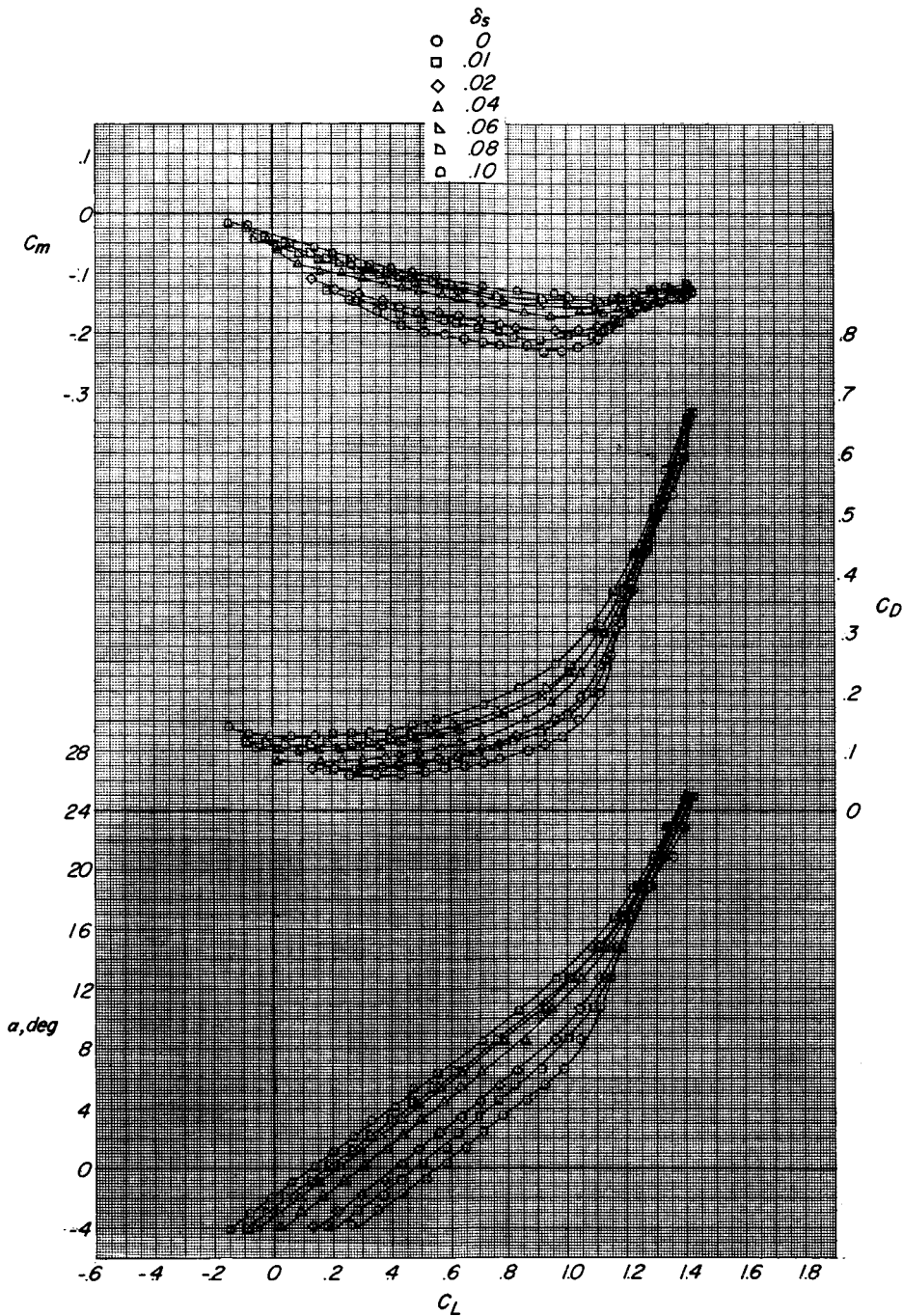


Figure 8.- Effect of deflections of three types of trailing-edge flaps on the longitudinal aerodynamic characteristics for typical landing conditions.  $\Lambda = 25^\circ$ ;  $\delta_n = -20^\circ$ .

L-1527

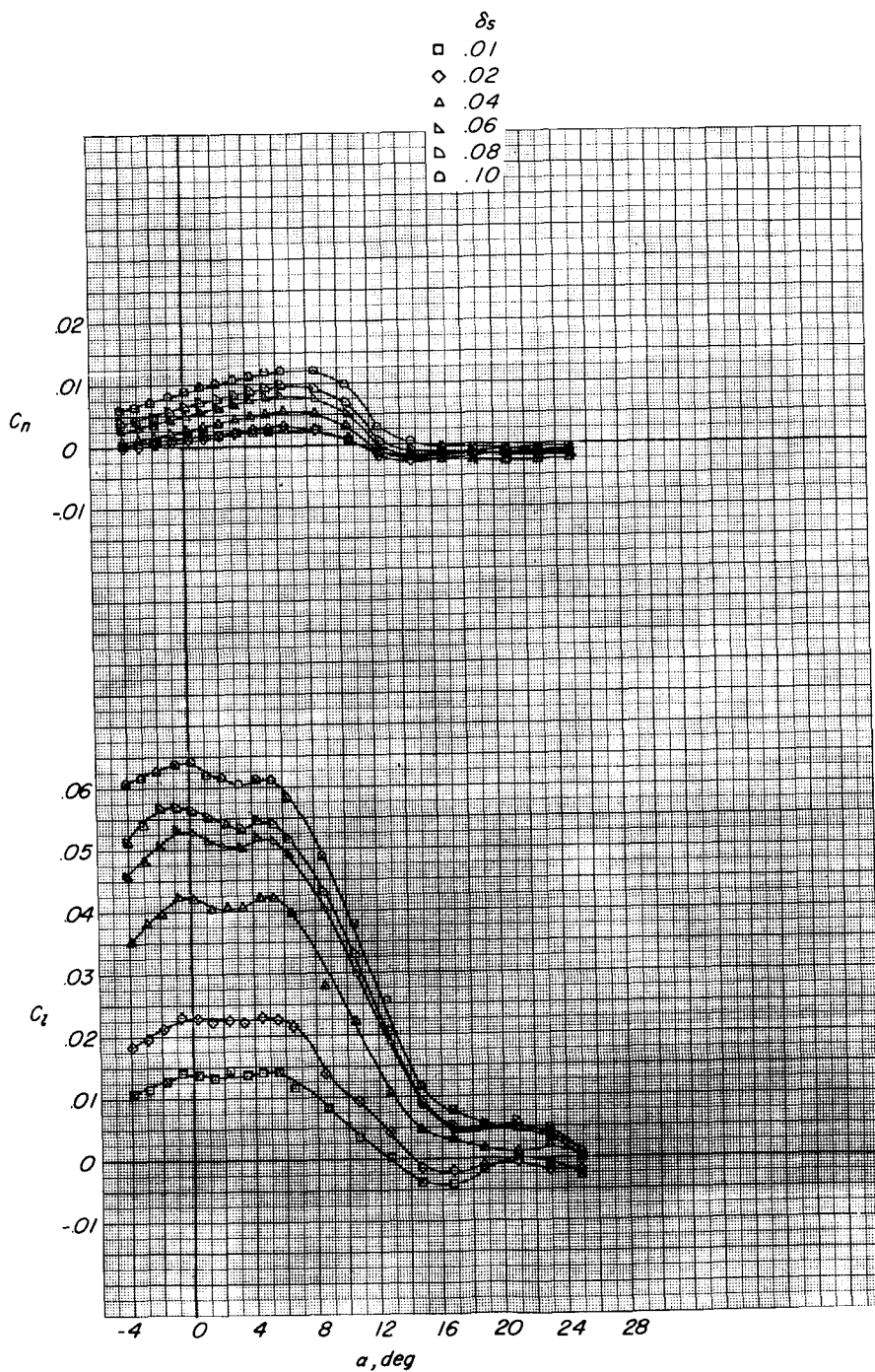


(a) Longitudinal.

Figure 9.- Effect of spoiler projections on the aerodynamic characteristics for various lateral control projections.  $\Lambda = 25^\circ$ ;  $\delta_d = 0.02$ ;  $\delta_n = -20^\circ$ ;  $\delta_f = 35^\circ$ .



I-1527

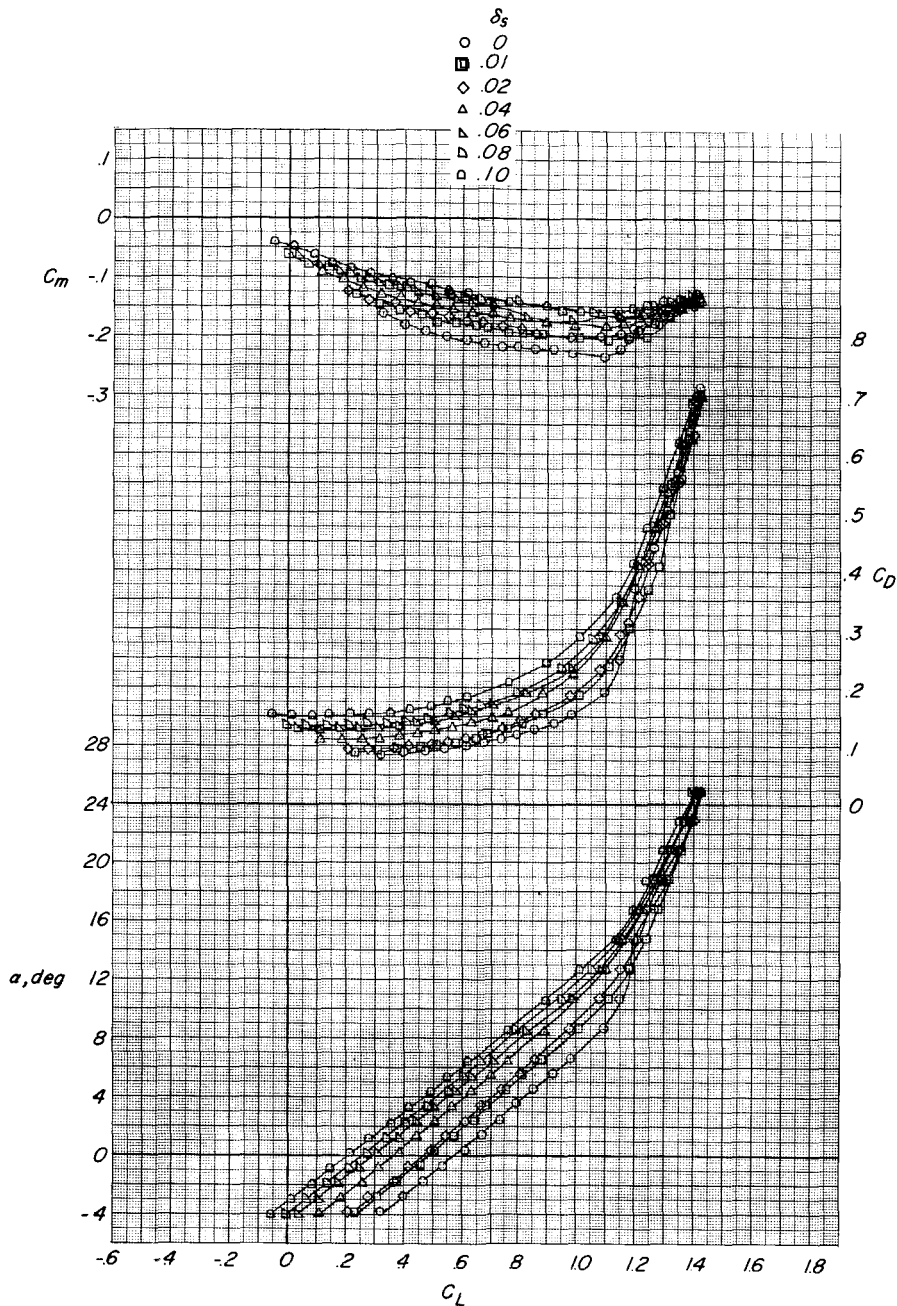


I-1527

(b) Lateral control.

Figure 9.- Concluded.

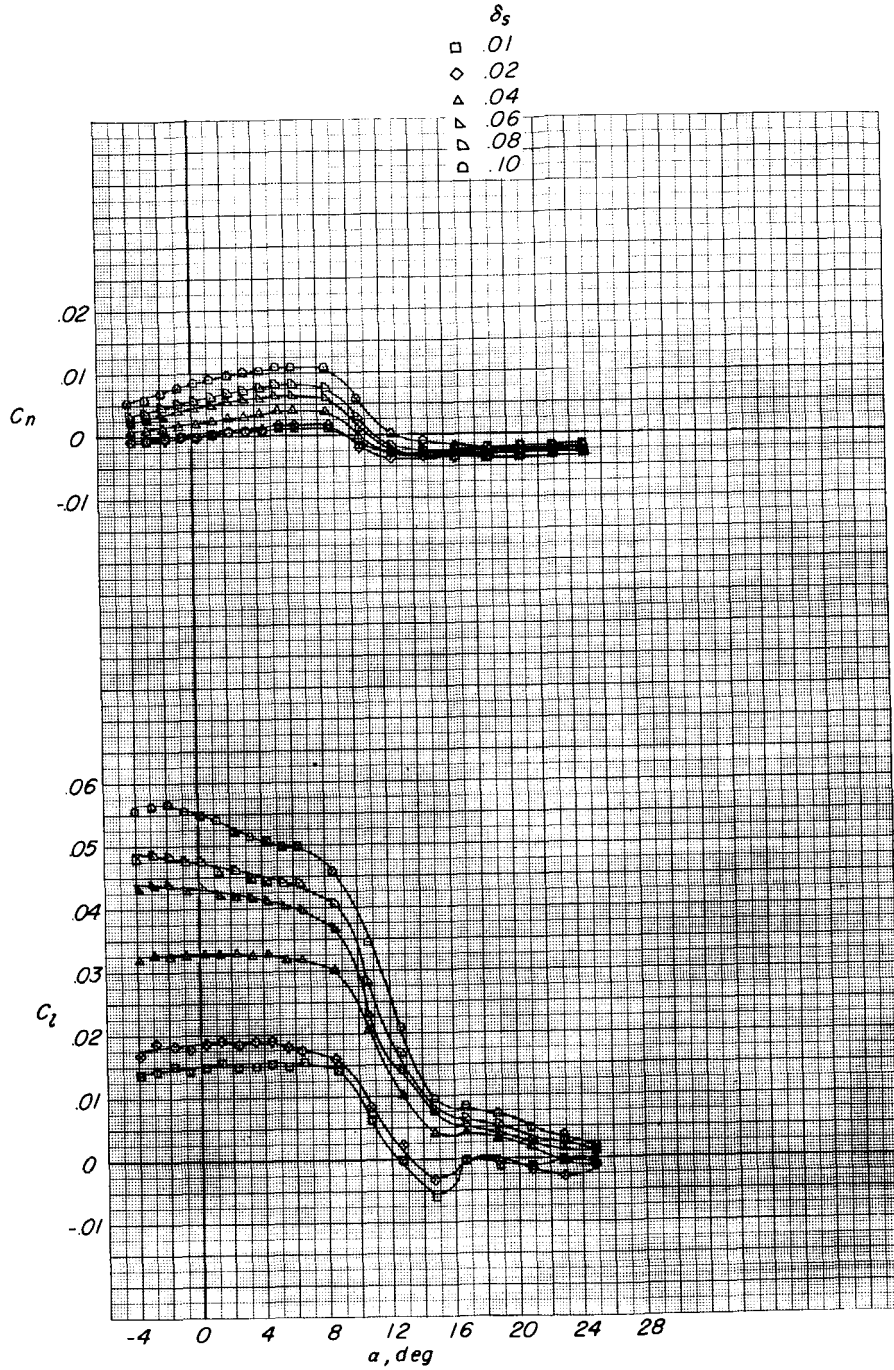




(a) Longitudinal.

Figure 10.- Effect of spoiler projections on the aerodynamic characteristics for various lateral control projections.  $\Lambda = 25^\circ$ ;  $\delta_d = 0.02$ ;  $\delta_n = -20^\circ$ ;  $\delta_f = 45^\circ$ .

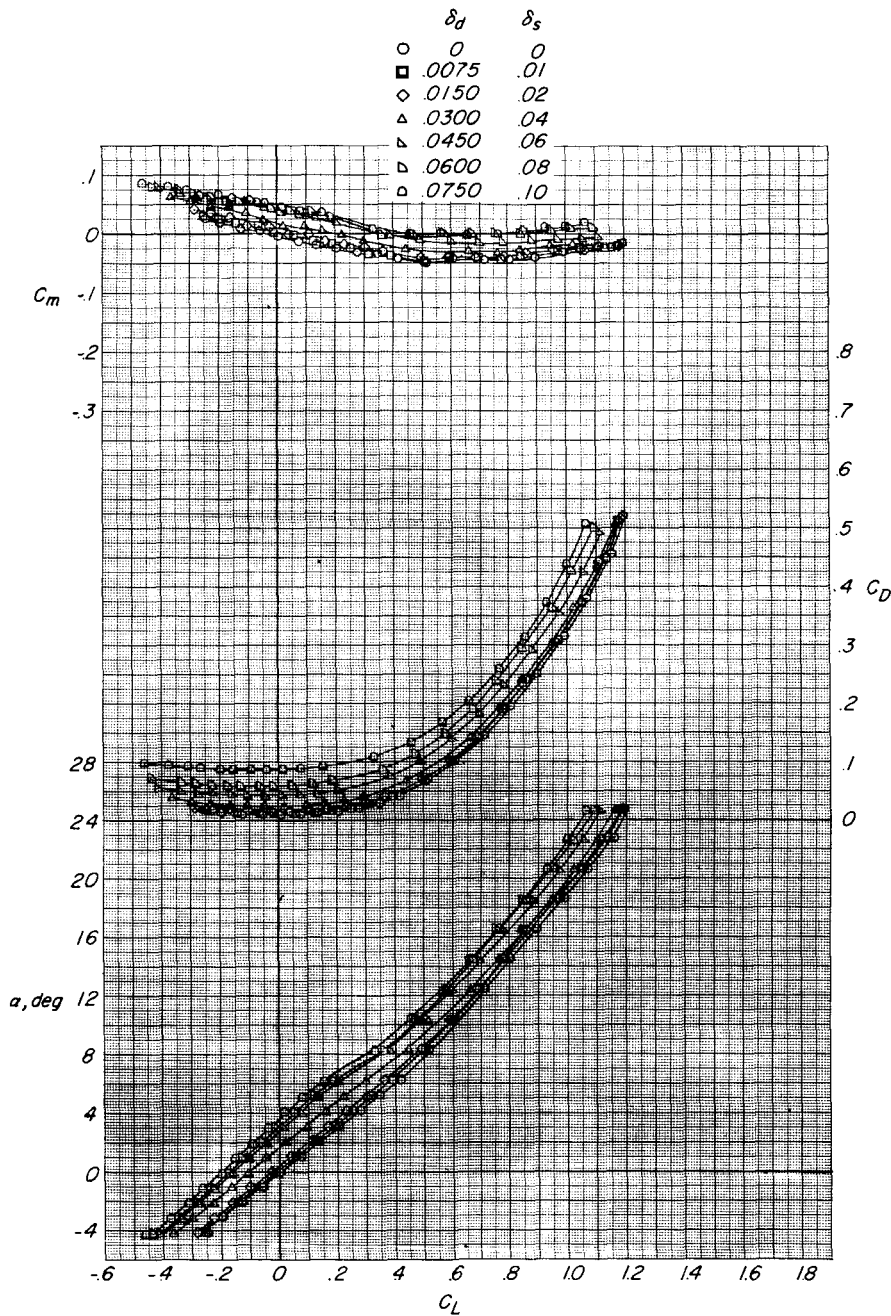




(b) Lateral control.

Figure 10.- Concluded.



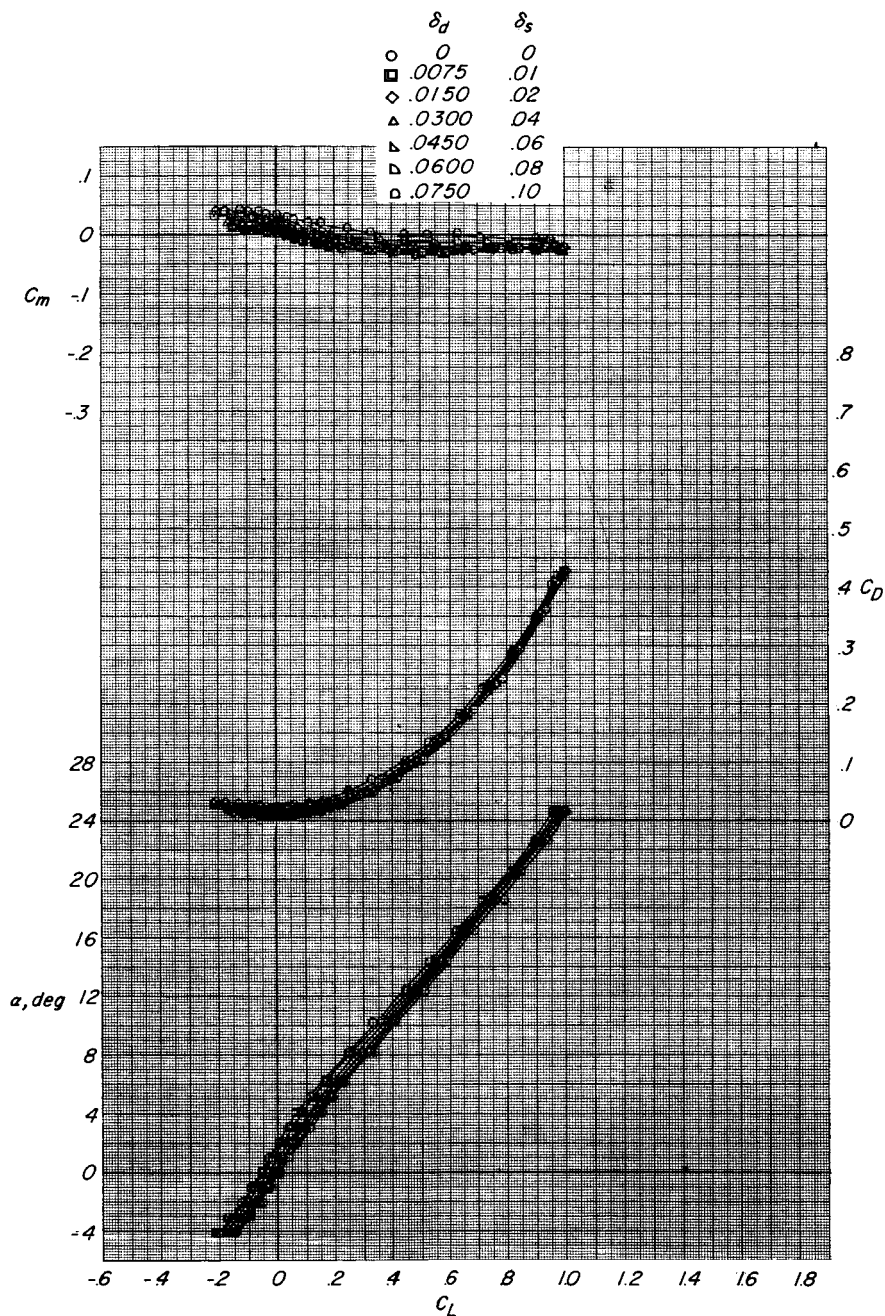


(a) Longitudinal.

Figure 11.- Effect of spoiler and deflector projections on the aerodynamic characteristics for various lateral control projections.  
 $\Lambda = 25^\circ$ ;  $\delta_n = 0^\circ$ ;  $\delta_f = 0^\circ$ .

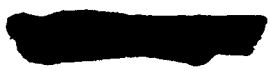


L-1527



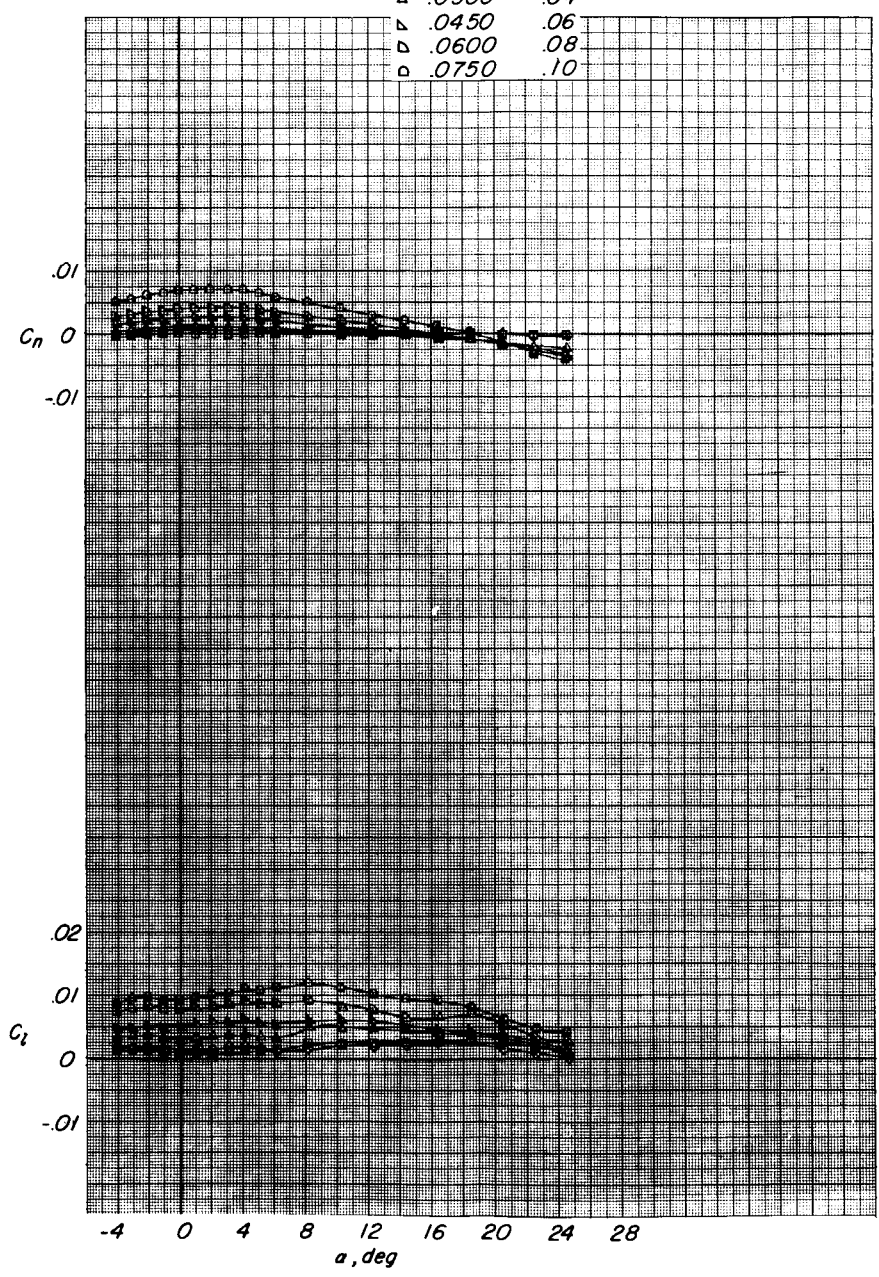
(a) Longitudinal.

Figure 12.- Effect of spoiler and deflector projections on the aerodynamic characteristics for various lateral control projections.  $\Lambda = 75^\circ$ ;  $\delta_n = 0^\circ$ ;  $\delta_f = 0^\circ$ .





	$\delta_d$	$\delta_s$
■	.0075	.01
◇	.0150	.02
△	.0300	.04
▽	.0450	.06
▷	.0600	.08
◁	.0750	.10



(b) Lateral control.

Figure 12.- Concluded.

